

## Answers to the first Referee R1.

We want to thank Dr. Baumgardner to review our study and making comments that allow to improve our manuscript.

Legend of styles

- **Reviewer comment**
- Author's answer
- (R1#i): flag to relate the change in the new manuscript (see author's comment)
- "*Change in the manuscript*"

**1) In the introduction and conclusions the authors emphasize the importance of dynamics on the cloud properties, then there is a very brief analysis of vertical velocity but after that section, no further effort is made to link microphysical properties to vertical velocity. In addition, given that updrafts are usually associated with hydrometeor growth and downdrafts with cloud decay, lumping all the results together regardless of vertical velocity direction will mask possibly important trends. The analysis has to include stratification by updraft and downdraft.**

The topic of stratification of our results as function of vertical velocity (updraft and downdraft) comes back often in the comment by reviewer R1. We reply here to all the comments linked to this topic.

Before presenting our results, the variability of the parameters as function of vertical movement and their intensity have been studied. However, no real tendencies have been identified that would allow to present our results also as function of updraft and downdraft.

Hence, parameterization or stratification of microphysical properties in MCS as function of vertical velocity (up and down) is not possible (with our in-situ dataset). However, in a first order, our study investigates variability of bulk microphysical properties of the icy part of MCS as function of temperature ranges and Z ranges (i.e. MCS reflectivity zones). If, no clear tendencies have been found as function of vertical velocities, we decide to investigate the probability to observe a vertical movement as function of Z (or MCS reflectivity zones). This work is discussed in section 3.2 with data from RASTA only; which contains much more data than in-situ measurement (more than a million of points versus about 53000 points for in-situ measurement). Then, the conclusion of this section is that the probability to observe vertical movement (updraft or downdraft) tend to increase with MCS reflectivity zones (or Z at constant altitude).

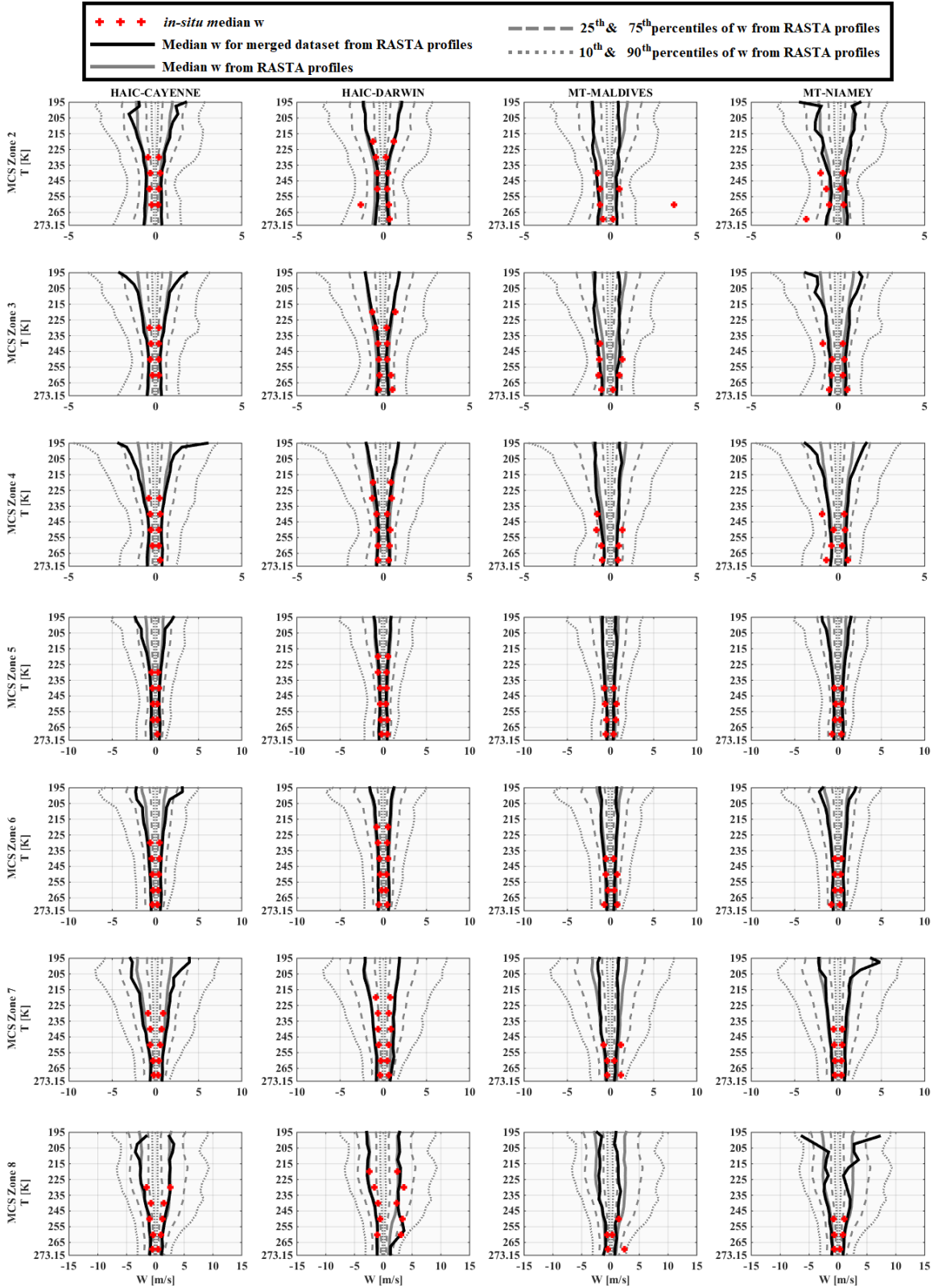
**Line 27 page 5: Why are you using absolute values?**

and

**Line 1 page 6: This does not seem reasonable to me to use absolute values as there is a very large difference between updrafts or downdrafts when it comes to storm dynamics and precipitation development.**

and

**Line 20 page 6: Somewhere it needs to be emphasized the significance of the updraft versus downdraft zones as they relate to the microphysical properties.**



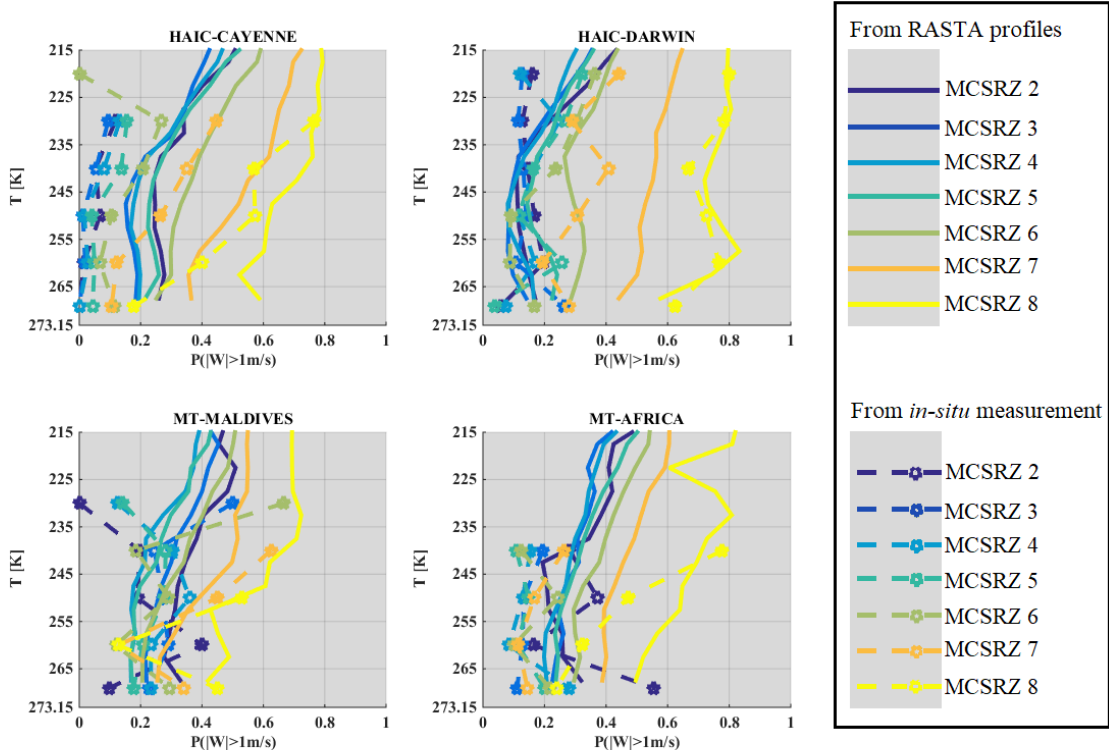
**Figure R 1: from the top line to the bottom line vertical velocities for MCSRZ 2 to MCSRZ 8.**

Figure R 1 shows median updraft and downdraft in each MCS reflectivity zones (MCSRZ 2 to MCSRZ 8 from the top line to the bottom line respectively) and for each airborne campaign (Cayenne, Darwin, Maldives Island and Niamey, from left column to right column respectively). Black lines represent median updraft and downdraft for each respective airborne campaigns, while grey lines are median (solid line), 25<sup>th</sup> and 75<sup>th</sup> percentiles (dashed

lines) and 10<sup>th</sup> and 90<sup>th</sup> percentiles (dotted lines) for the merged dataset. Black lines and grey lines are calculated using RASTA vertical profiles. The red stars are median downdraft and updraft when taken only vertical movement measured by the aircraft (in-situ measurement).

We can see that median updraft and median downdraft for each airborne campaigns from in-situ and RASTA measurement agree well with median updraft and downdraft for the merged dataset in each MCSRZ. Also, we can observe a symmetry between updraft and downdraft in all MCS reflectivity zones for each campaigns, meaning that at a given altitude, absolute magnitude of downdraft is about the magnitude of updraft for median, 25<sup>th</sup>, 75<sup>th</sup>, 10<sup>th</sup> and 90<sup>th</sup> calculated percentiles.

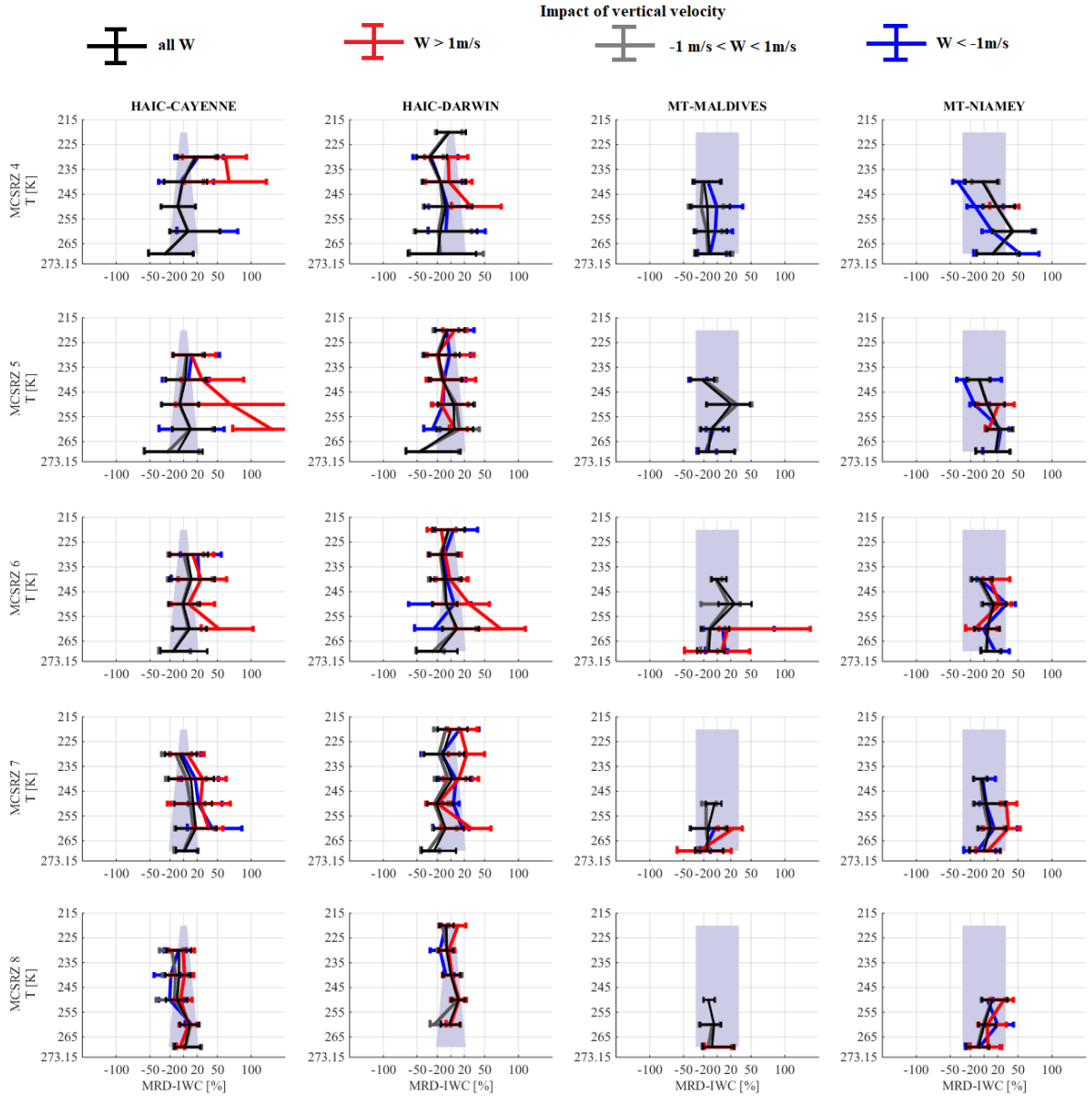
The decision of taking a threshold of 1m/s for updraft and downdraft, is motivated by the fact that we have to take into account the measurement uncertainty (less than 0.5m/s). Moreover, knowing that variance of vertical turbulences are about 1.5 m<sup>2</sup>/s<sup>2</sup> (Large Eddy Simulations at 50 m resolution; personal communication with Dr. R. Didier). We take roughly a value of 1m/s to be the threshold to detect vertical movement, such -1m/s < w < 1m/s there is no noticeable vertical movement neither upward nor downward. Hence, investigating the probability to observe vertical movement with an absolute magnitude larger than 1m/s seems reasonable to determine which MCS reflectivity zones have a higher probability to be linked to a convective area.



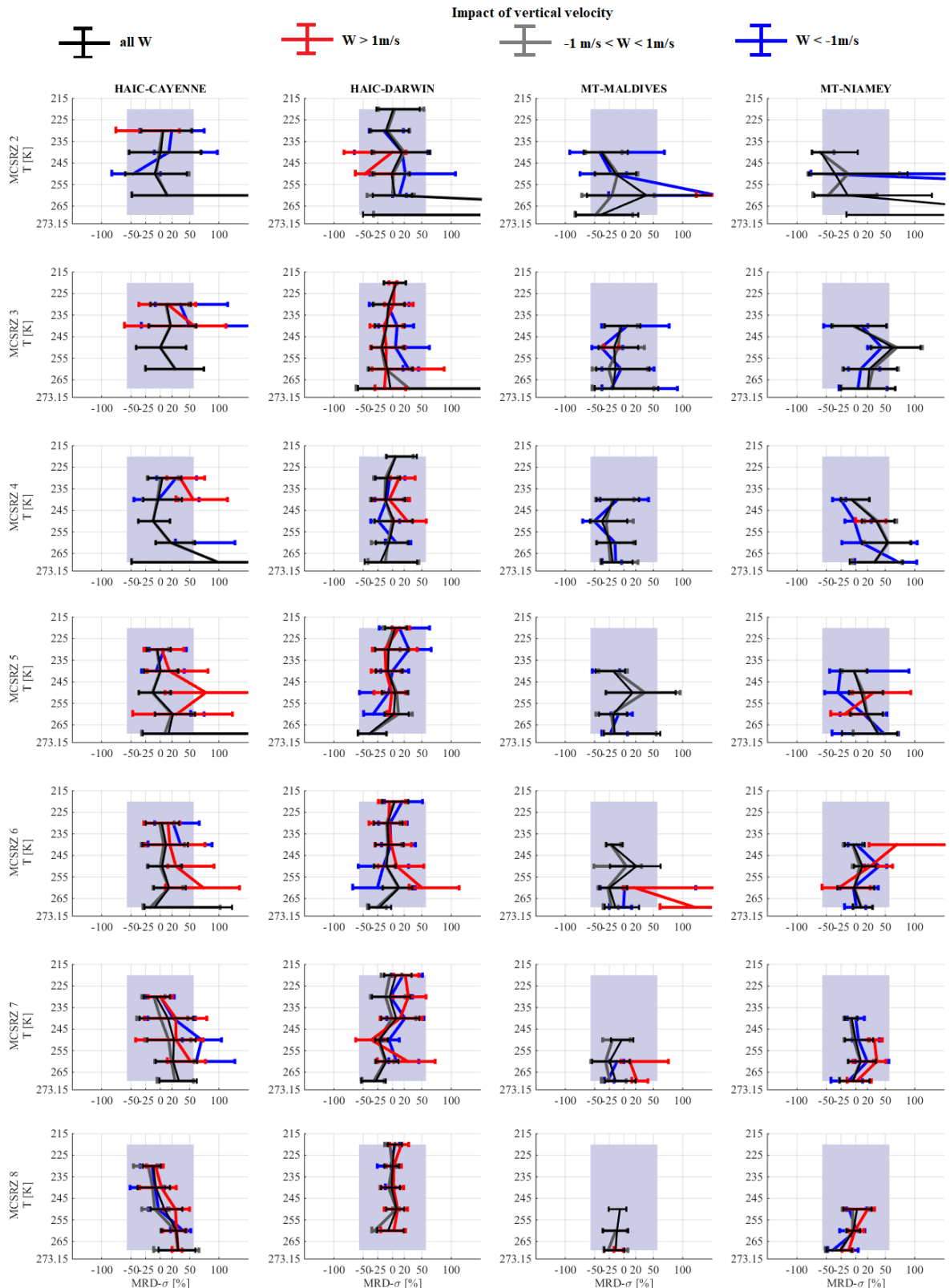
**Figure R 2 : Probability to observe vertical velocity with absolute magnitude larger than 1m/s in each MCS reflectivity zone (MCSRZ; color scale) for measurement from the radar Doppler RASTA in solid lines and in dashed lines with stars marker for in-situ measurement.**

Figure R 2, is similar to Figure 3 in our reviewed study. It shows probability to observe vertical movement with magnitude larger than 1m/s in each MCS reflectivity zones (solid lines). Solid lines in Figure R 2 are probabilities calculated from RASTA measurement and dashed lines with stars are probabilities calculated with w measured at the flight level. Both type of probabilities are different in each MCS zones and probabilities made with in-situ measurement are smaller than these calculated with RASTA retrievals; except in MCS reflectivity zones 8 in Darwin where they are similar. From there, we know from the point of view of vertical velocity that the in-situ dataset is not similar to the dataset from RASTA retrievals: different probability to observe vertical velocity with magnitude larger than 1m/s (updraft and downdraft).

Impact of vertical velocity on Median relative differences:



**Figure R 3 : Median relative difference of IWC (MRD-IWC) with regards to median IWC calculated for the merged dataset in each MCS reflectivity zone (Figure 5-a). Results are sorted as function of MCSRZ 4 (top line) to MCSRZ 8 bottom line. Blue lines represent MRD-IWC for vertical velocity smaller than -1m/s. Grey lines represent MRD-IWC for vertical velocity larger than -1m/s and smaller than 1m/s. Red lines represent MRD-IWC for vertical velocity larger 1m/s. The black lines represent MRD-IWC when there is no distinction as function of vertical velocity (same as in Figure 5-b, c, d, e).**



**Figure R 4 : Median relative difference of extinction (MRD- $\sigma$ ) with regards to median extinction calculated for the merged dataset in each MCS reflectivity zone (Figure 6-a). Results are sorted as function of MCSRZ 2 (top line) to MCSRZ 8 bottom line. Blue lines represent MRD-  $\sigma$  for vertical velocity smaller than  $-1\text{ m/s}$ . Grey lines represent MRD-  $\sigma$  for vertical velocity larger than  $-1\text{ m/s}$  and smaller than  $1\text{ m/s}$ . Red lines represent MRD-  $\sigma$  for vertical velocity larger  $1\text{ m/s}$ . The black lines represent MRD-  $\sigma$  when there is no distinction as function of vertical velocity (same as in Figure 6-b, c, d, e).**

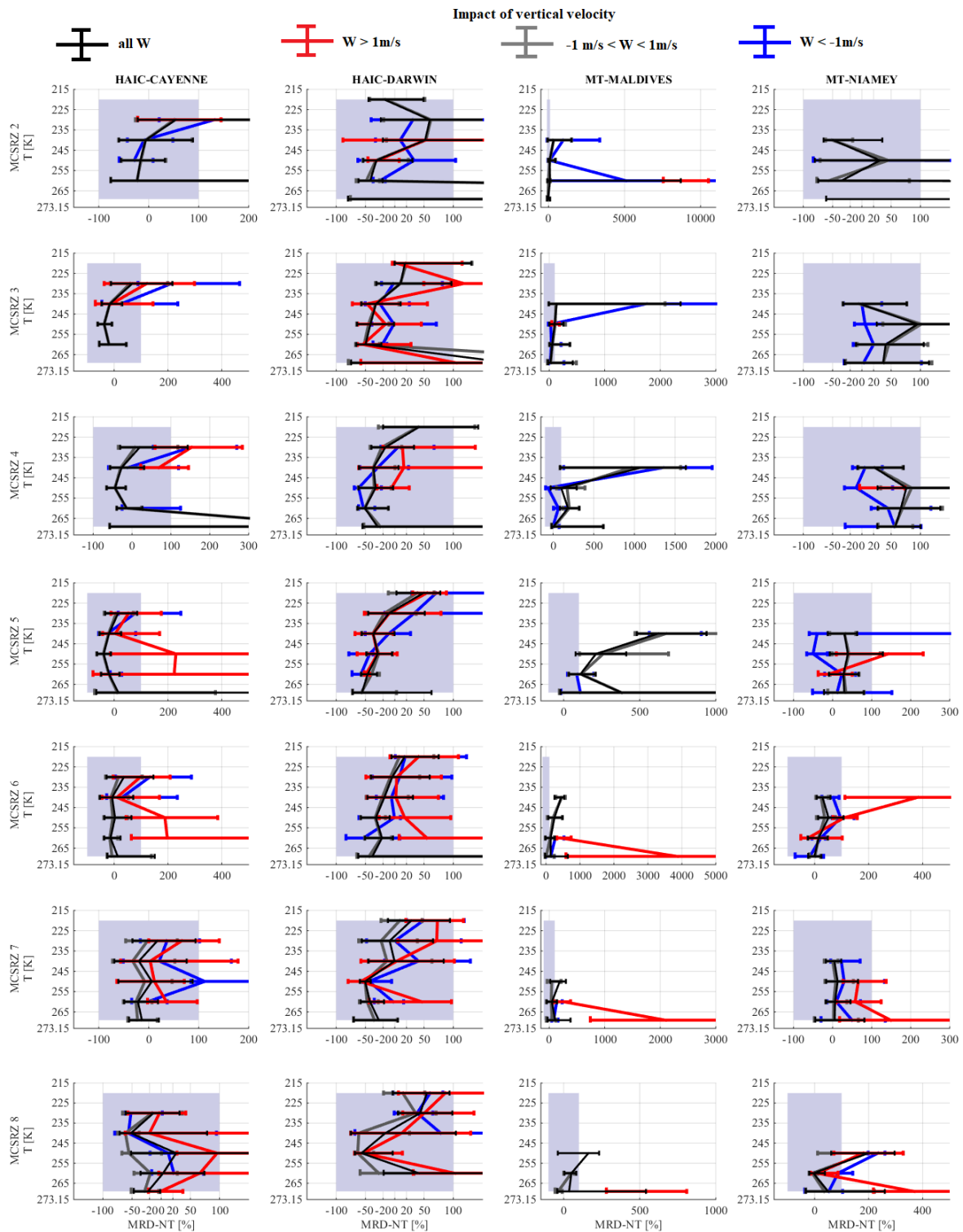


**Figure R 5 : Median relative difference of total concentration of hydrometeors (MRD-NT) with regards to median total concentrations calculated for the merged dataset in each MCS reflectivity zone (Figure 8-a).** Results are sorted as function of MCSRZ 2 (top line) to MCSRZ 8 bottom line. Blue lines represent MRD-NT for vertical velocity smaller than -1m/s. Grey lines represent MRD-NT for vertical velocity larger than -1m/s and smaller than 1m/s. Red lines represent MRD-NT for vertical velocity larger 1m/s. The black lines represent MRD-NT when there is no distinction as function of vertical velocity (same as in Figure 8-b, c, d, e).

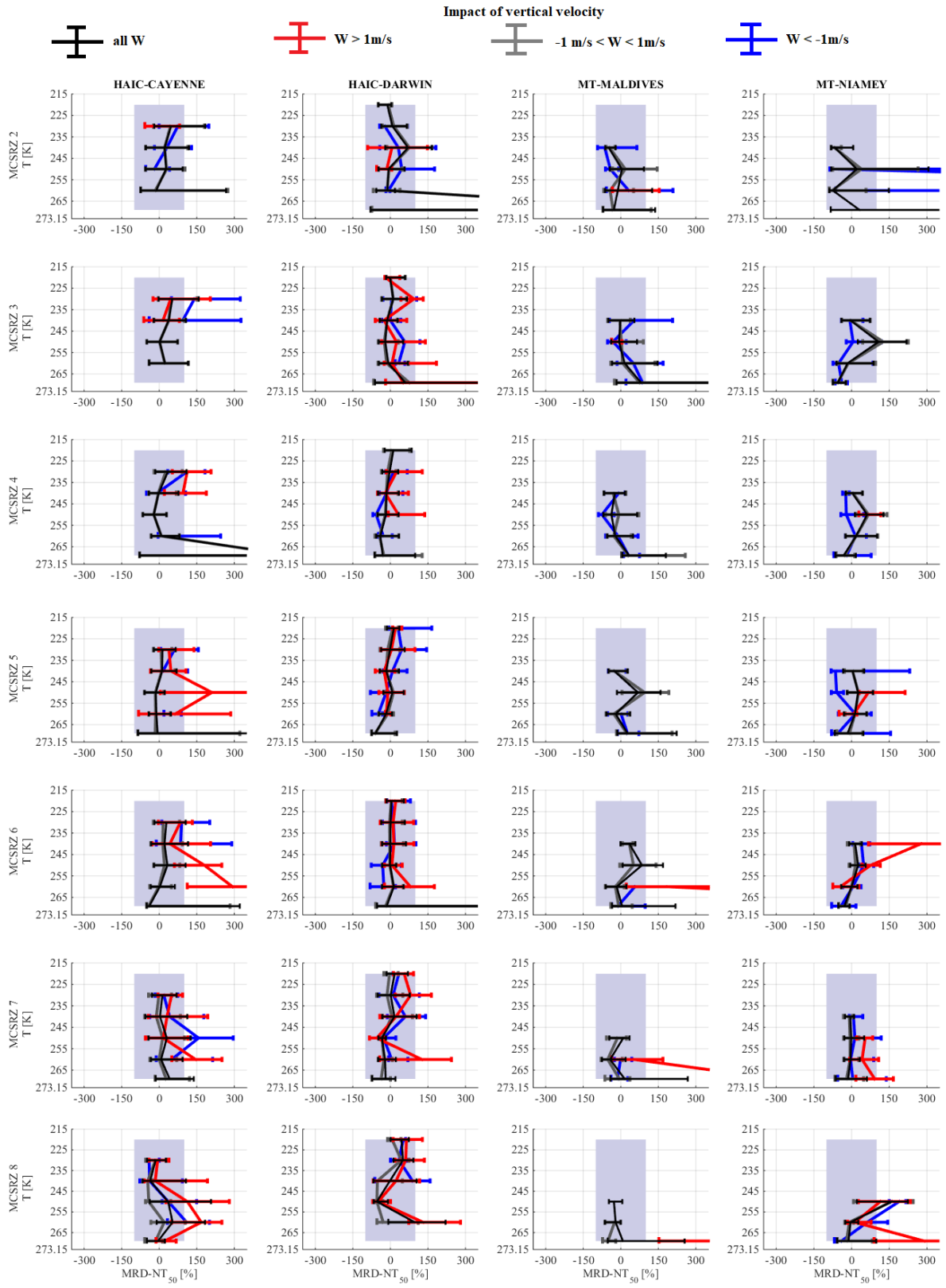


**Figure R 6 : Median relative difference of concentration of hydrometeors summed over Dmax for Dmax larger than 50µm (MRD-NT<sub>50</sub>) with regards to median total concentrations calculated for the merged dataset in each MCS reflectivity zone (Figure 9-a). Results are sorted as function of MCSRZ 2 (top line) to MCSRZ 8 bottom line. Blue lines represent MRD-NT<sub>50</sub> for vertical velocity smaller than -1m/s. Grey lines represent MRD-NT<sub>50</sub> for vertical velocity larger than -1m/s and smaller than 1m/s. Red lines represent**

**MRD-NT<sub>50</sub> for vertical velocity larger 1m/s. The black lines represent MRD-NT<sub>50</sub> when there is no distinction as function of vertical velocity (same as in Figure 9-b, c, d, e).**

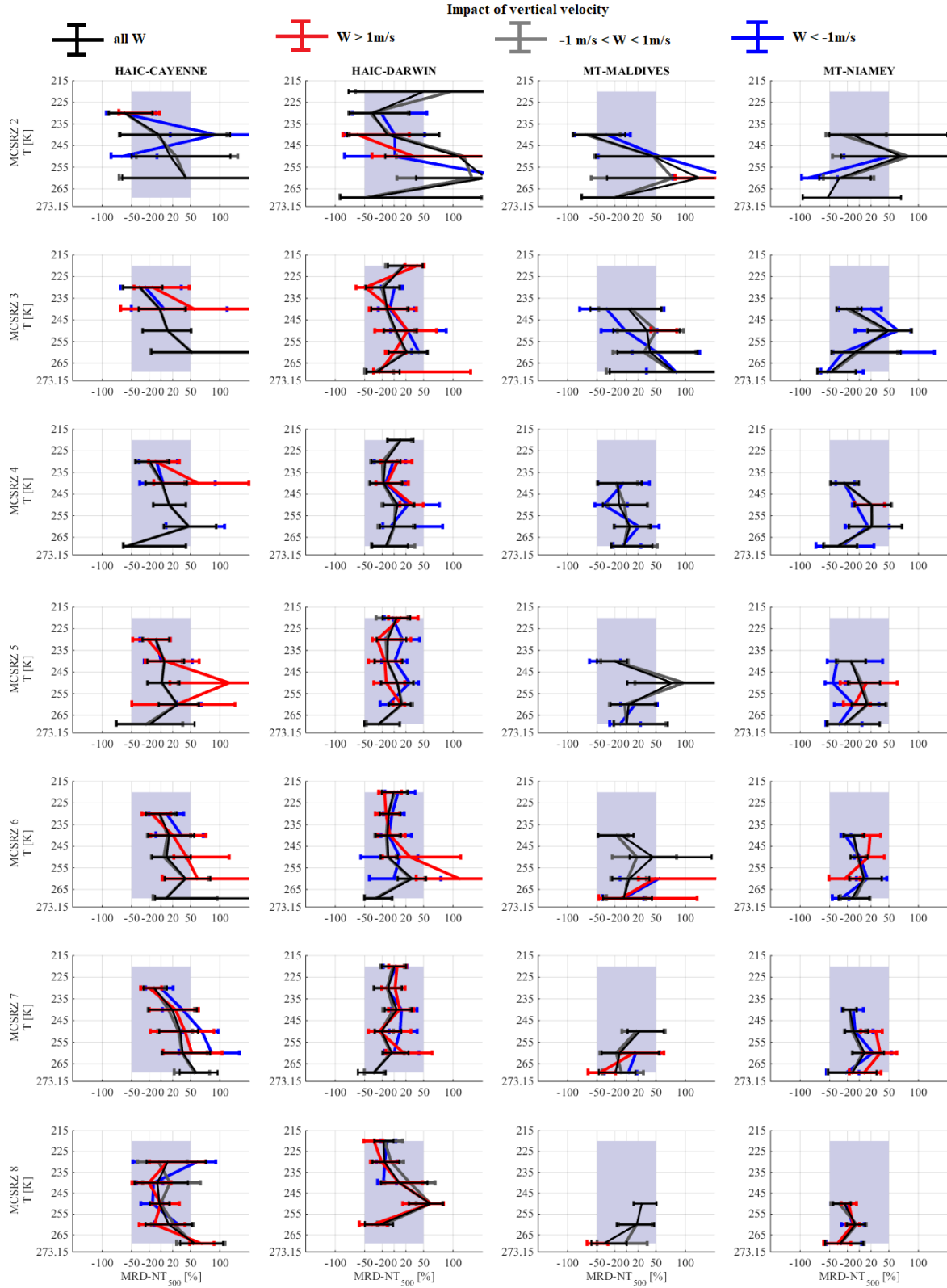


**Figure R 7 : Median relative difference of concentration of hydrometeors summed over Dmax for Dmax larger than 500μm (MRD-NT<sub>500</sub>) with regards to median total concentrations calculated for the merged dataset in each MCS reflectivity zone (Figure 10-a). Results are sorted as function of MCSRZ 2 (top line) to**

**MCSRZ 8 bottom line.** Blue lines represent MRD-NT<sub>500</sub> for vertical velocity smaller than -1m/s. Grey lines represent MRD-NT<sub>500</sub> for vertical velocity larger than -1m/s and smaller than 1m/s. Red lines represent MRD-NT<sub>500</sub> for vertical velocity larger 1m/s. The black lines represent MRD-NT<sub>500</sub> when there is no distinction as function of vertical velocity (same as in Figure 10-b, c, d, e).

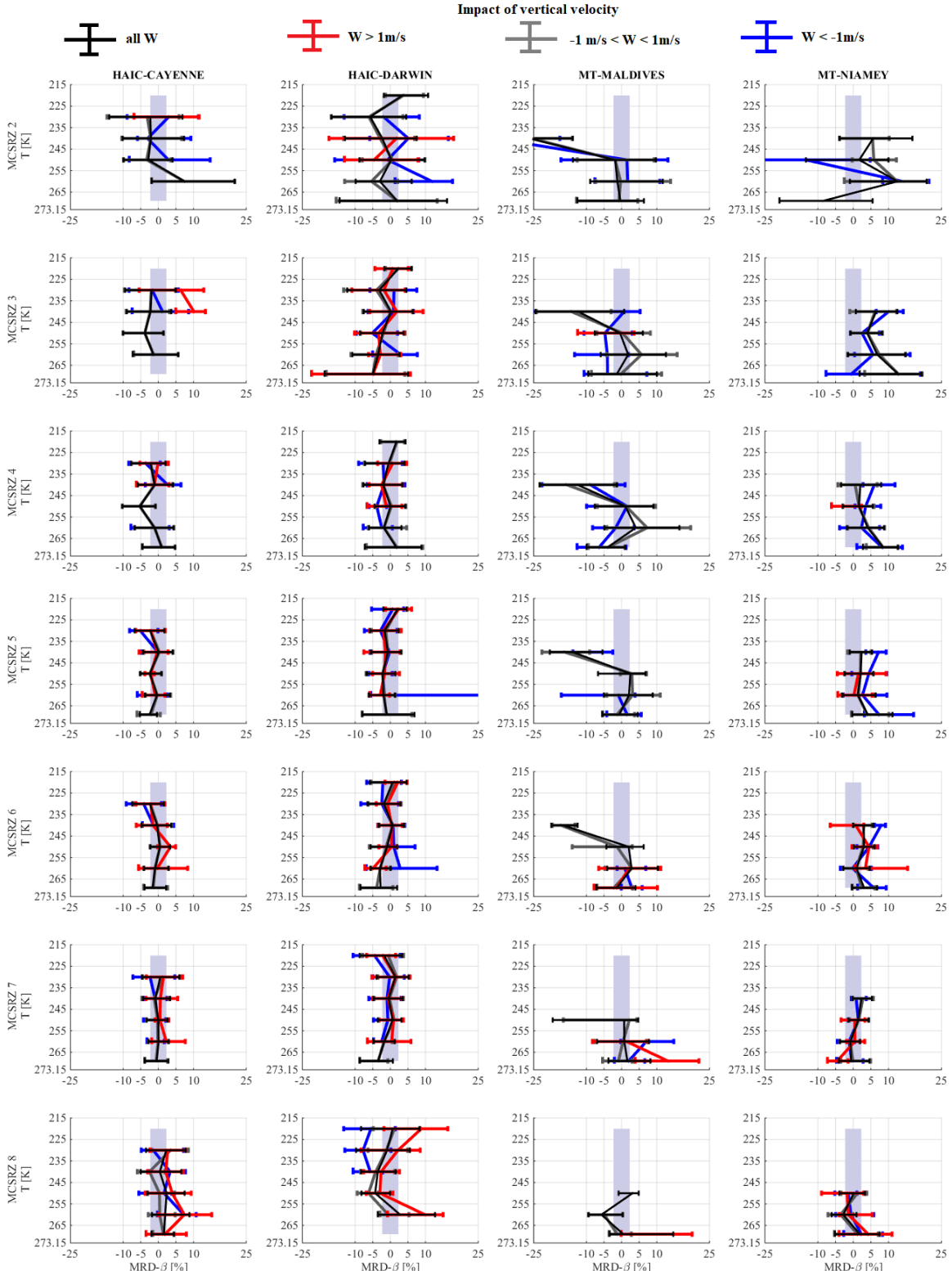


**Figure R 8 : Median relative difference of the exponent of mass-size relationship  $\beta$  (MRD- $\beta$ ) with regards to median  $\beta$  calculated for the merged dataset in each MCS reflectivity zone (Figure 11-a). Results are sorted**

as function of MCSRZ 2 (top line) to MCSRZ 8 bottom line. Blue lines represent MRD- $\beta$  for vertical velocity smaller than -1m/s. Grey lines represent MRD- $\beta$  for vertical velocity larger than -1m/s and smaller than 1m/s. Red lines represent MRD- $\beta$  for vertical velocity larger 1m/s. The black lines represent MRD- $\beta$  when there is no distinction as function of vertical velocity (same as in Figure 11-b, c, d, e).

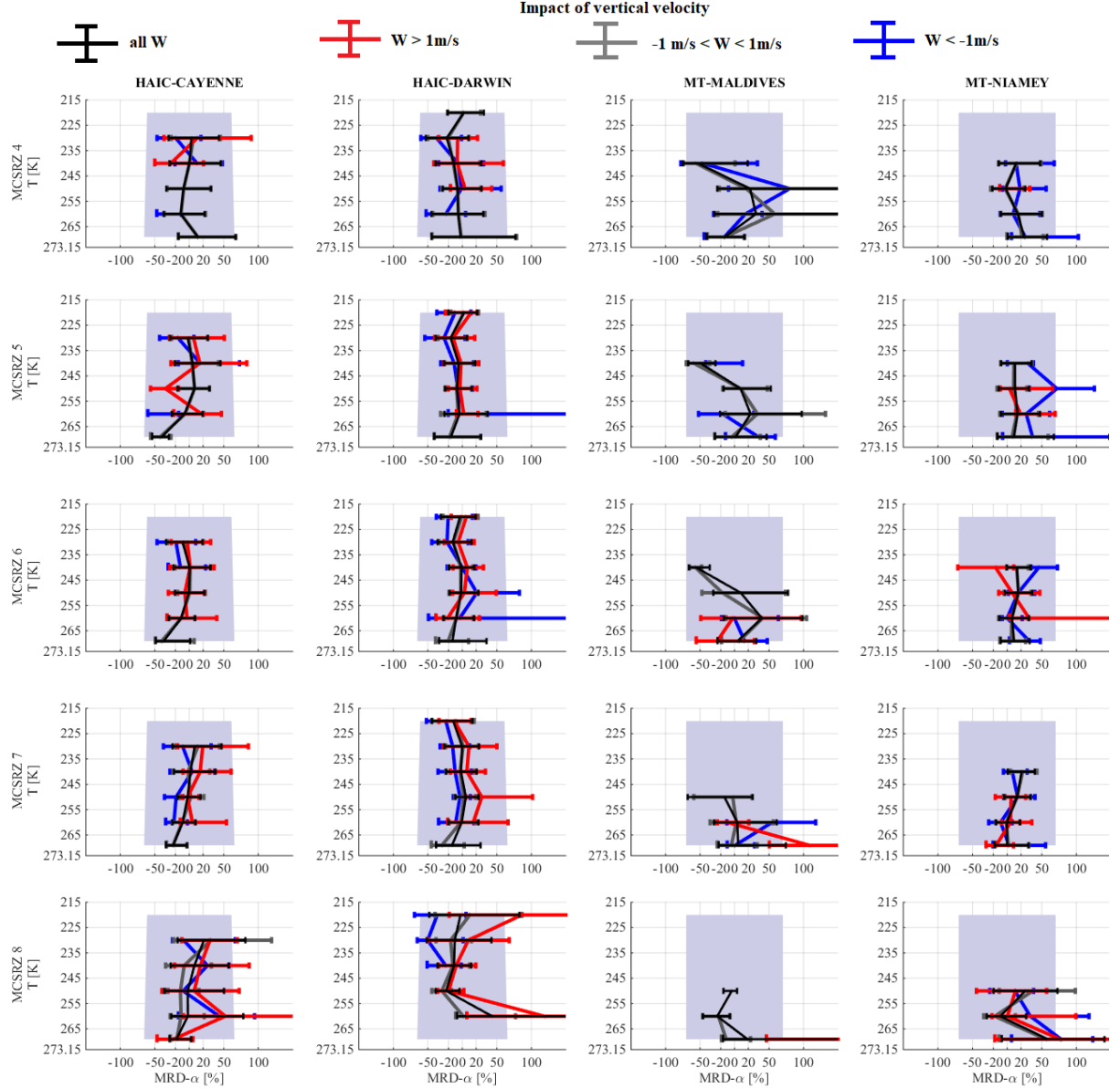


**Figure R 9 :** Median relative difference of the pre-factor of mass-size relationship  $\alpha$  (MRD- $\alpha$ ) with regards to median  $\alpha$  calculated for the merged dataset in each MCS reflectivity zone (Figure 12-a). Results are sorted as function of MCSRZ 4 (top line) to MCSRZ 8 bottom line. Blue lines represent MRD- $\alpha$  for vertical velocity smaller than -1m/s. Grey lines represent MRD- $\alpha$  for vertical velocity larger than -1m/s and smaller than 1m/s. Red lines represent MRD- $\alpha$  for vertical velocity larger 1m/s. The black lines represent MRD- $\alpha$  when there is no distinction as function of vertical velocity (same as in Figure 12-b, c, d, e).

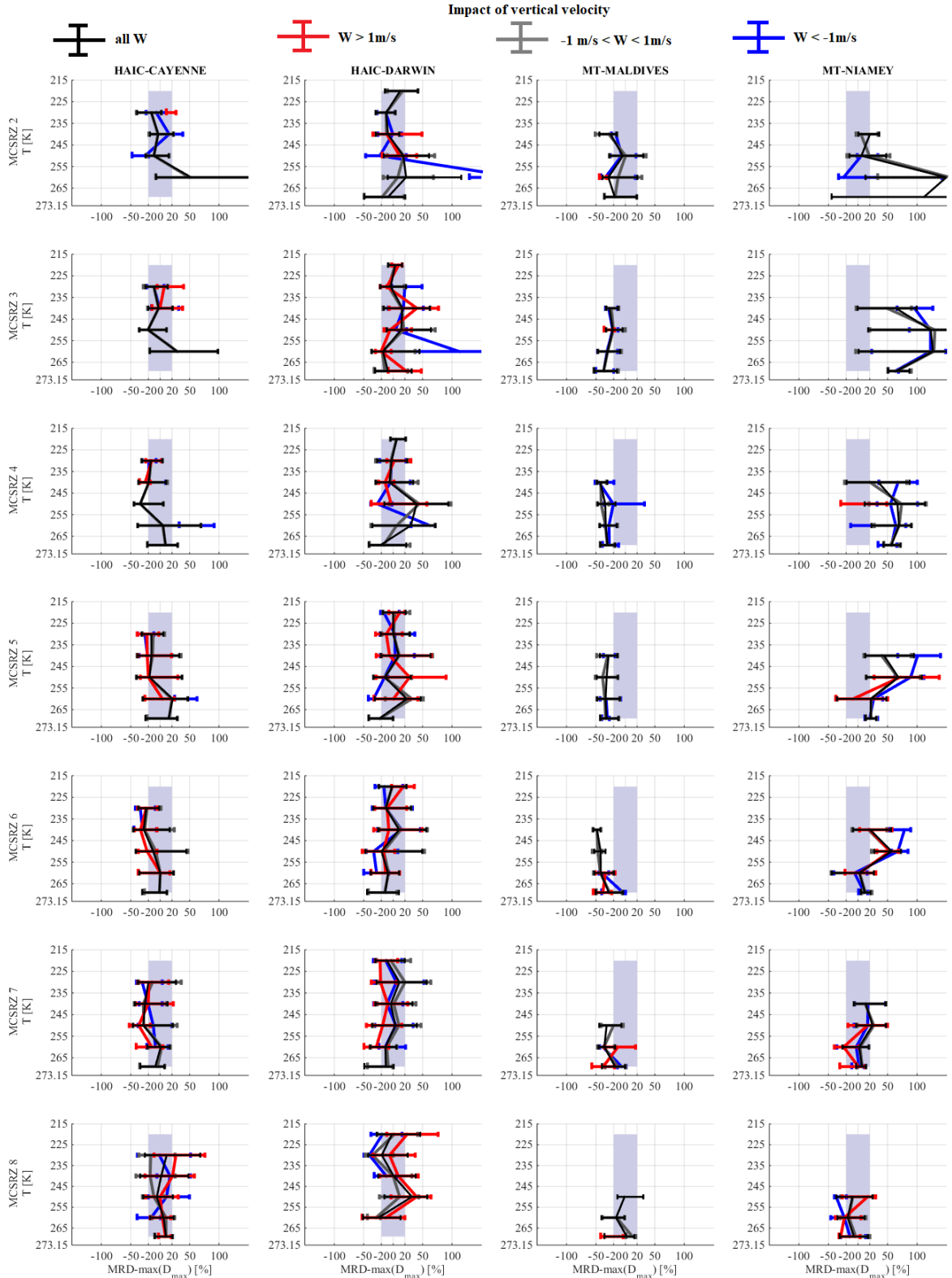


**Figure R 10 :** Median relative difference of size of larger hydrometeors in PSD (MRD-max( $D_{\max}$ )) with regards to median max( $D_{\max}$ ) calculated for the merged dataset in each MCS reflectivity zone (Figure 13-a). Results are sorted as function of MCSRZ 2 (top line) to MCSRZ 8 bottom line. Blue lines represent MRD-max( $D_{\max}$ ) for vertical velocity smaller than -1m/s. Grey lines represent MRD-max( $D_{\max}$ ) for vertical velocity larger than -1m/s and smaller than 1m/s. Red lines represent MRD-max( $D_{\max}$ ) for vertical velocity larger 1m/s. The black lines represent MRD-max( $D_{\max}$ ) when there is no distinction as function of vertical velocity (same as in Figure 13-b, c, d, e).

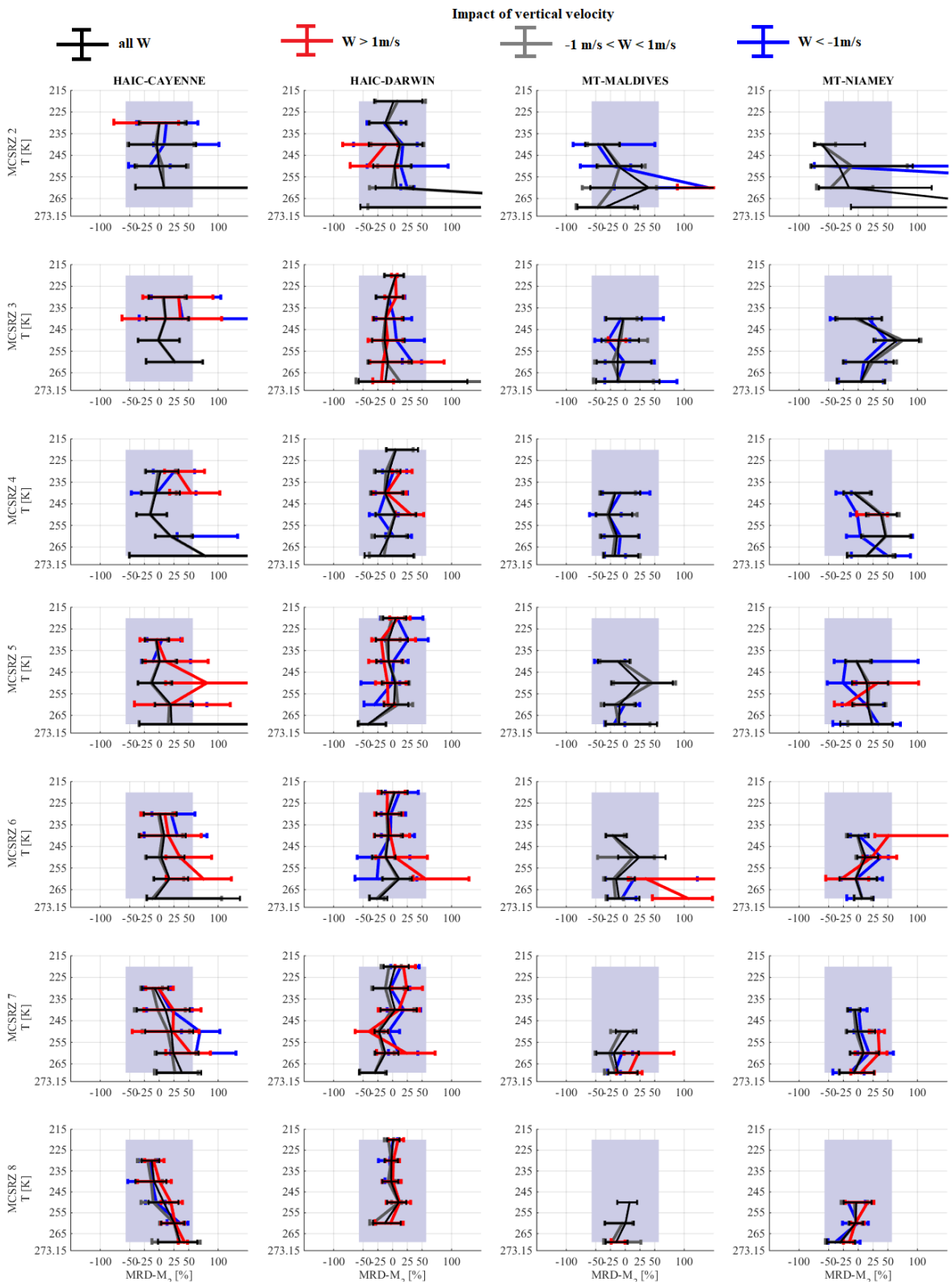


**Figure R 11:** Median relative difference of second moment of PSD  $M_2$  (MRD- $M_2$ ) with regards to median  $M_2$  calculated for the merged dataset in each MCS reflectivity zone (Figure 14-a). Results are sorted as function of MCSRZ 2 (top line) to MCSRZ 8 bottom line. Blue lines represent MRD- $M_2$  for vertical velocity smaller than -1m/s. Grey lines represent MRD- $M_2$  for vertical velocity larger than -1m/s and smaller than

**1m/s. Red lines represent MRD-M<sub>2</sub> for vertical velocity larger 1m/s. The black lines represent MRD-M<sub>2</sub> when there is no distinction as function of vertical velocity (same as in Figure 14-b, c, d, e).**

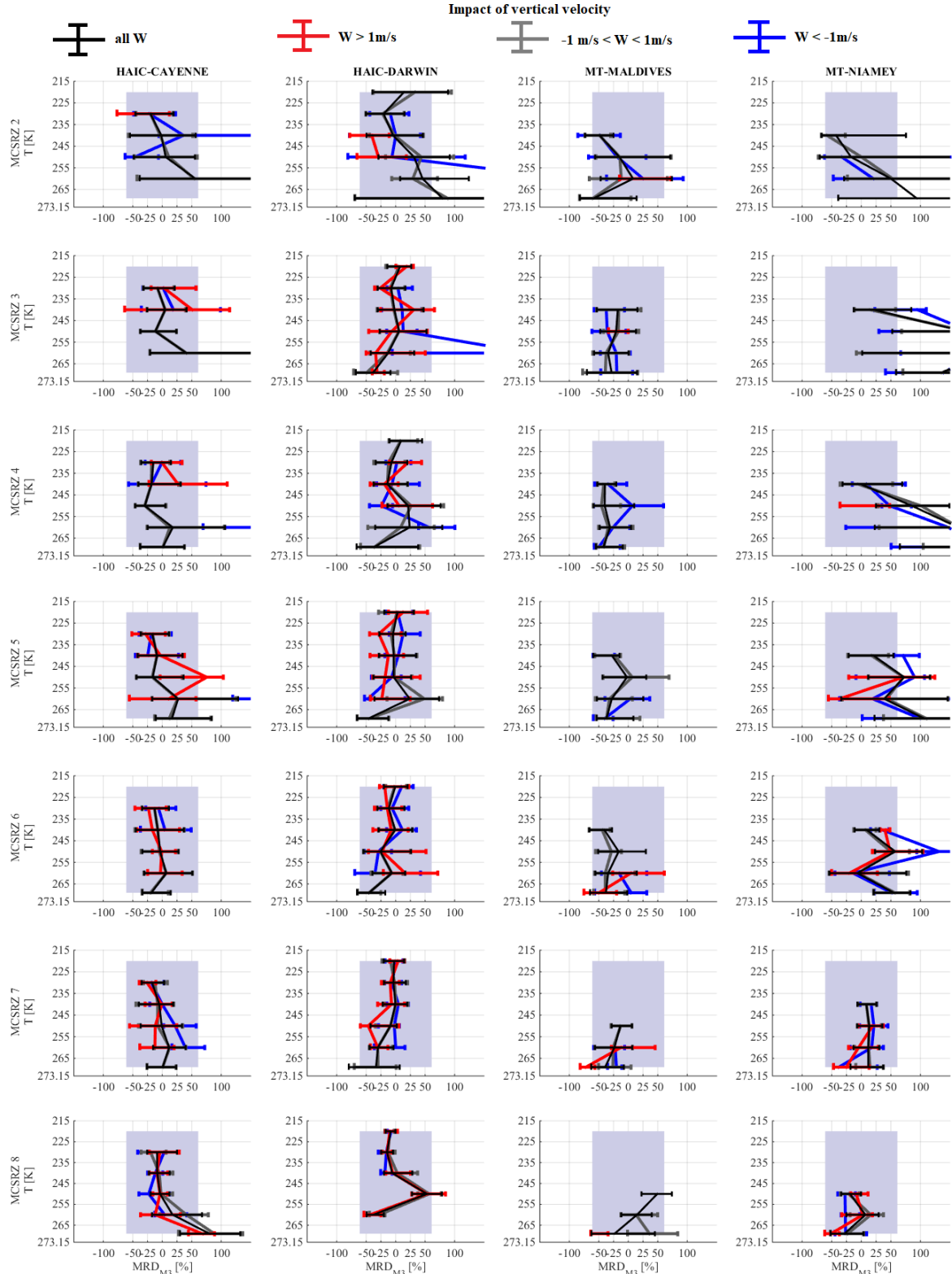


**Figure R 12: Median relative difference of third moment of PSD M<sub>3</sub> (MRD-M<sub>3</sub>) with regards to median M<sub>3</sub> calculated for the merged dataset in each MCS reflectivity zone (Figure 14-a). Results are sorted as function of MCSRZ 2 (top line) to MCSRZ 8 bottom line. Blue lines represent MRD-M<sub>3</sub> for vertical velocity smaller than -1m/s. Grey lines represent MRD-M<sub>3</sub> for vertical velocity larger than -1m/s and smaller than 1m/s. Red**

lines represent MRD-M<sub>3</sub> for vertical velocity larger 1m/s. The black lines represent MRD-M<sub>3</sub> when there is no distinction as function of vertical velocity (same as in Figure 15-b, c, d, e).

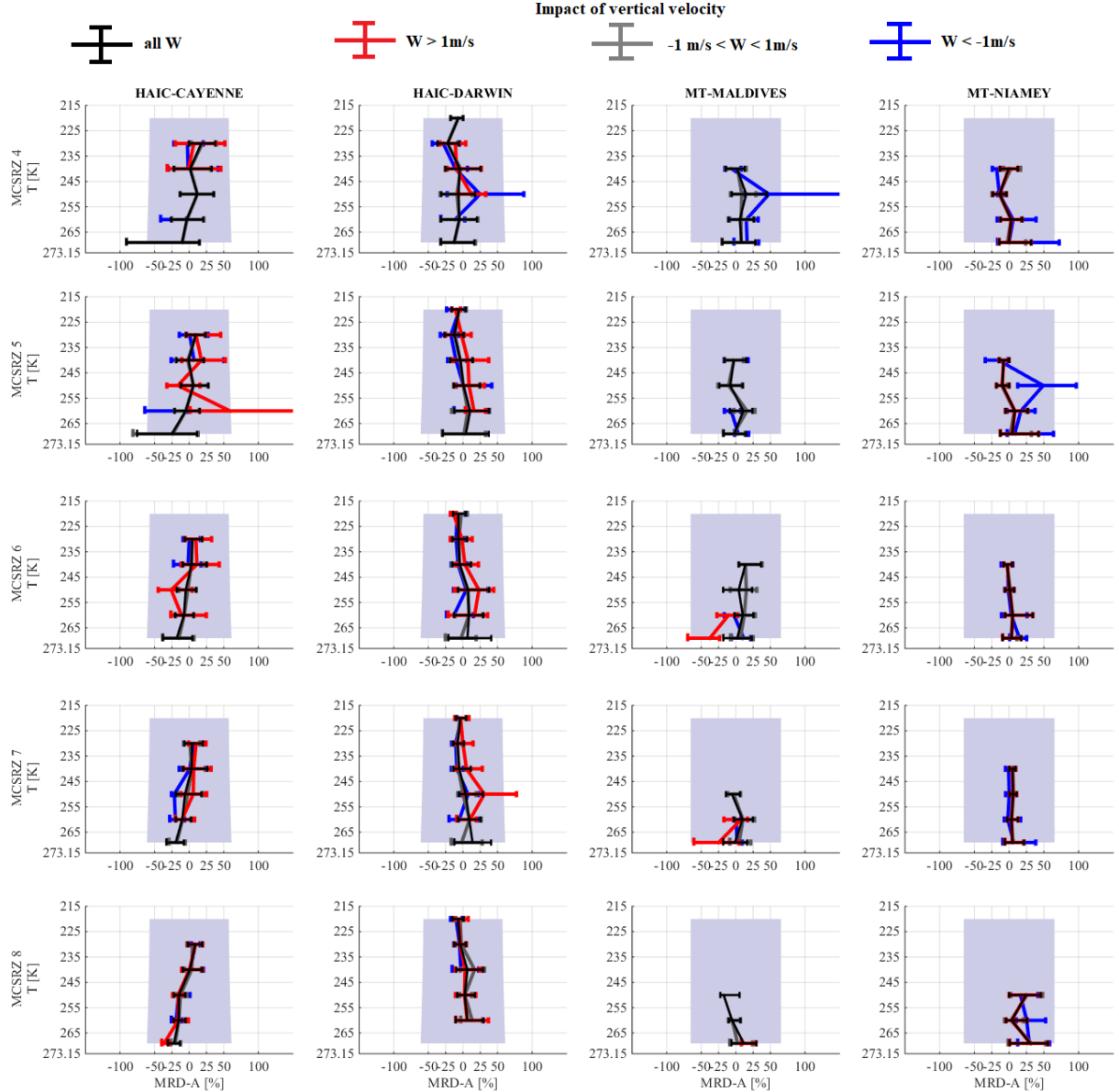


**Figure R 13 : Median relative difference of the ratio A(=IWC/M2; MRD-A) with regards to median A calculated for the merged dataset in each MCS reflectivity zone (Figure 16-a). Results are sorted as function of MCSRZ 4 (top line) to MCSRZ 8 bottom line. Blue lines represent MRD-A for vertical velocity smaller than -1m/s. Grey lines represent MRD-A for vertical velocity larger than -1m/s and smaller than 1m/s. Red lines represent MRD-A for vertical velocity larger 1m/s. The black lines represent MRD-A when there is no distinction as function of vertical velocity (same as in Figure 16-b, c, d, e).**

Figure R 3 to Figure R 13 show the median relative difference of the studied parameters X (MRD-X; X being used to replace IWC,  $\sigma$ , NT, NT50, NT500,  $\beta$ ,  $\alpha$ , max(Dmax), M2, M3 and A=IWC/M2) with regards to the median of the X parameter in each MCS reflectivity zones. These figures shows 4 types of MRD-X: (i) MRD-X when  $w < -1\text{m/s}$  (downdraft:  $w < 0\text{m/s}$ ; blue lines), (ii) MRD-X when  $-1\text{m/s} < w < 1\text{m/s}$  ( $w \approx 0\text{m/s}$ ; grey lines), (iii) MRD-X when  $w > 1\text{m/s}$  (updraft:  $w > 0\text{m/s}$ ; red lines) and (iv) MRD-X when  $w$  is not considered (black lines; merged dataset).

Firstly, we can notice that MRD-X for  $w \approx 0\text{m/s}$  (grey lines) are similar to MRD-X for the merged dataset (black line), showing that impact of downdraft and updraft have nearly no impact on the median tendencies calculated for each microphysical parameters presented in our study. Secondly, there are few differences between MRD-X

for downdraft and MRD-X for the merged dataset (black line). However, these differences are not significant compared to uncertainties of each microphysical parameters ( $U(X)/X$ ; grey bands).

Concerning the impact of updraft on microphysical parameters (red lines), there are some noticeable differences, where MRD-X for updraft are larger than MRD-X for the merged dataset and larger than  $U(X)/X$ . It appears that updraft tends to impact mainly concentrations of small hydrometeors and IWC for some type of MCS and some MCS reflectivity zones. So for NT (Figure R5), we observe larger NT for updraft in MCS observed over Cayenne, Maldives and Niamey. For Cayenne, it appears in MCS reflectivity zone 5 and 6 for temperatures between 245K and 265 K with NT 2 to 3 times larger than NT for merged dataset. For MCS over Maldives, median NT are 5 times to 20 times larger than NT when there is no noticeable vertical movement in MCS reflectivity zones 6, 7 and 8. Finally for MCS over Niamey, we observe larger NT in updraft than NT for the merged dataset in MCS reflectivity zones 6 for T around 240 K and in MCS reflectivity zones 8 above the bright band. We have similar conclusions for  $NT_{50}$  (Figure R6), except that ratio between  $NT_{50}$  in updraft and  $NT_{50}$  when no updraft is smaller than the ratio between NT in updraft and NT when no updraft.

IWC are impacted by updraft only for MCS over Cayenne, in MCS reflectivity zone 4, 5, 6 and 7. IWC in updraft tend to be larger about +50% than IWC when no updraft, except in MCS reflectivity zones where IWC are about 2 times larger in updraft than IWC when no updraft.

This investigation on the impact of updraft and downdraft on ice microphysics, shows that updraft may have an impact on concentrations of small hydrometeors and IWC. However, updraft does not impact all type of MCS in the same way. So, there is a need to performed deeper investigations on updraft impact.

Despites some noticeable impact of updraft on ice microphysic for our dataset, there is not significant (recurrence trough all types of MCS or as function of T or Z) results to assess them for the merged dataset. So we cannot add a stratification of our results as function of updraft and downdraft, as for the parameterizations provided in our study.

Page 2 line 27 (R1#1).

*“Investigations on the impact of vertical velocity has been performed asides, however no significant tendencies were found to allow us to present our results as function of vertical velocity.”*

Page 2 line 36 (R1#2).

*“The third section presents the analysis of radar reflectivity factors (Z) which provides the ranges of Z to perform the intercomparison between the four types of MCS. Moreover, for each range of Z a statistical analysis of vertical velocity is presented to bind the vertical dynamic of MCS and ice microphysical properties. The section 4 present the methodology of intercomparison used in this study. And section 5, present the inter-comparison of the microphysical parameters as function of Z and T. The end of this section is dedicated to present shortly the results of the investigations performed about the impact of vertical velocity. The sixth section, provide the parameterization of visible extinction and the parameterization of ice hydrometeors distributions. The last section adds the discussion and conclusion.”*

We propose to re-write the sub-section 3.2 (R1#3)

“

### 3.2 Retrieved vertical velocity in MCS reflectivity zones

This section investigates links between retrieved vertical velocity and MCS reflectivity zones. We assume that  $V_z (V_d) = w_{ret} + V_t$ , where  $V_t$  is the terminal velocity of hydrometeors (Delanoë et al., 2007, 2014) and  $w_{ret}$  the vertical wind speed. In a first order, our study investigates variability of bulk microphysical properties of the icy part of MCS as function of temperature range and Z range (i.e. MCS reflectivity zones). As no clear tendencies have been found as function of vertical velocities, we decide to investigate the probability to observe significant vertical movement in each range of Z (or MCS reflectivity zones). In other words, we investigate if there is any relationship between MCS reflectivity zones and vertical dynamic of MCS. We assume that convective part of MCS are associated with pronounced updraft and downdraft and that stratiform part of MCS have non-pronounced vertical velocity ( $w \approx 0 \text{ m.s}^{-1}$ ) (see Figure 16 from Houze 2004).

Figure 3 shows median updraft ( $w_{ret} > 0$ ) and downdraft ( $w_{ret} < 0$ ) in each MCS reflectivity zones (MCSRZ 2 to MCSRZ 8 from the top line to the bottom line respectively) and for each airborne campaign (Cayenne, Darwin, Maldives Island and Niamey, from left column to right column respectively). Black lines represent median updraft

and downdraft for each respective airborne campaigns, while grey lines are median (solid line), 25<sup>th</sup> and 75<sup>th</sup> percentiles (dashed lines) and 10<sup>th</sup> and 90<sup>th</sup> percentiles (dotted lines) for the merged dataset. Black lines and grey lines are calculated using RASTA vertical profiles. The red stars are median downdraft and updraft when we use only vertical velocity measured by the aircraft ( $w$ ; in-situ measurement).

We can observe a symmetry between updraft and downdraft in all MCS reflectivity zones for each campaigns, meaning that at a given altitude, absolute magnitude of downdraft is about the magnitude of updraft for median, 25<sup>th</sup>, 75<sup>th</sup>, 10<sup>th</sup> and 90<sup>th</sup> calculated percentiles. For RASTA measurement, we can see that median updraft ( $w_{rel} > 0 \text{ m.s}^{-1}$ ) and median downdraft ( $w_{rel} < 0 \text{ m.s}^{-1}$ ) for each airborne campaigns agree well with median updraft and downdraft for the merged dataset in all MCS reflectivity zones. Except for Maldives observations where median  $w_{rel}$  are smaller for  $T < 255\text{K}$ . Also, median in-situ  $w$  tend to be a bit smaller than median  $w_{rel}$ , except for updraft in Maldives above the bright band;  $w \approx 2.5 \text{ m.s}^{-1}$  versus  $w_{rel} \approx 1 \text{ m.s}^{-1}$ .

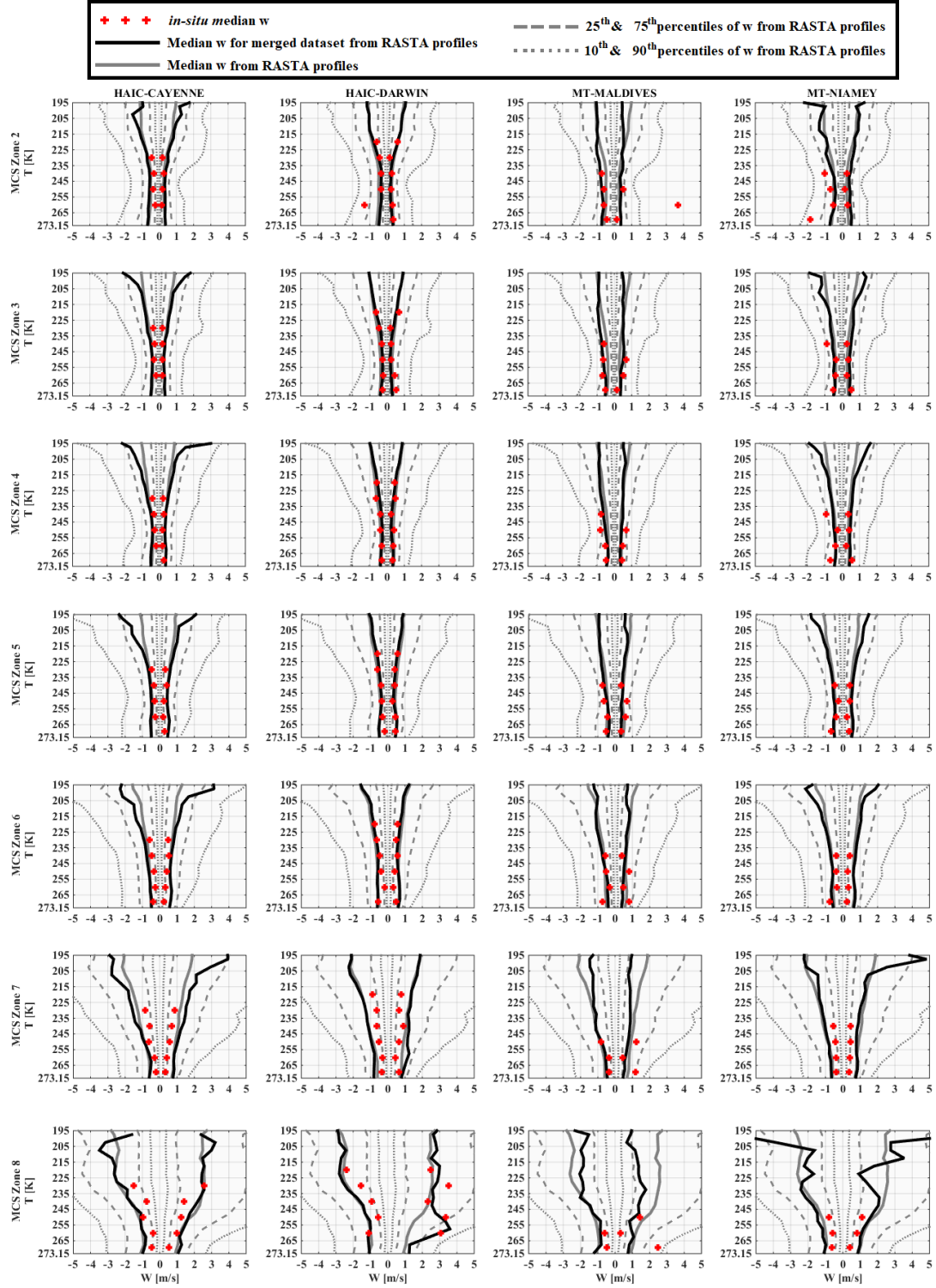


**Figure 3: from the top line to the bottom line vertical velocities for MCS reflectivity zone 2 to MCS reflectivity zone 8.**

In general the updraft and downdraft wind speeds increase with altitude and MCS reflectivity zones, where magnitudes of vertical velocity (negative and positive) are highest for MCS reflectivity zones 8. For all 4 datasets vertical wind speeds of MCS reflectivity zones 2-6 are smaller than  $1 \text{ m.s}^{-1}$ .

To complete our study on vertical dynamic that could exist in each MCS reflectivity zones, we study the probability to observe vertical movement. We use a threshold for vertical velocity to distinguish between discernible vertical movement and nearly not.

We take roughly a value of  $1\text{m/s}$  to be the threshold to detect vertical movement, such  $-1\text{m/s} < w < 1\text{m/s}$  there is no noticeable vertical movement neither upward nor downward. The decision of taking a threshold of  $1\text{m/s}$  for updraft and downdraft, is motivated by the fact that we have to take into account the measurement uncertainty (less than  $0.25\text{-}0.5\text{m.s}^{-1}$ ). Moreover, knowing that variance of vertical turbulences are about  $1.5\text{ m}^2/\text{s}^2$  (Large Eddy Simulations at  $50\text{ m}$  resolution; Strauss et al., 2019). The fact that median  $w_{\text{ret}}$  for the merged dataset in MCS reflectivity zones 2 to 6 are smaller than  $1\text{m.s}^{-1}$  consolidate our decision to take a threshold of  $1\text{m.s}^{-1}$ .

Then, knowing  $T$  and  $Z$ , a probability to observe  $|w_{\text{ret}}| \geq 1\text{m.s}^{-1}$  is calculated as a function of MCS reflectivity zones and temperature. Colored solid lines in Figure 4 are probabilities calculated from RASTA measurement and dashed lines with stars are probabilities calculated with vertical velocity measured at the aircraft level (in-situ measurement). Both type of probabilities are different in each MCS zones and probabilities made with in-situ measurement are smaller than these calculated with RASTA retrievals; except in MCS reflectivity zones 8 in Darwin where they are similar. Hence, we know from the point of view of vertical velocity that the in-situ dataset is not representative to the observations from RASTA retrievals: different probability to observe vertical velocity with magnitude larger than  $1\text{m/s}$  (updraft and downdraft).

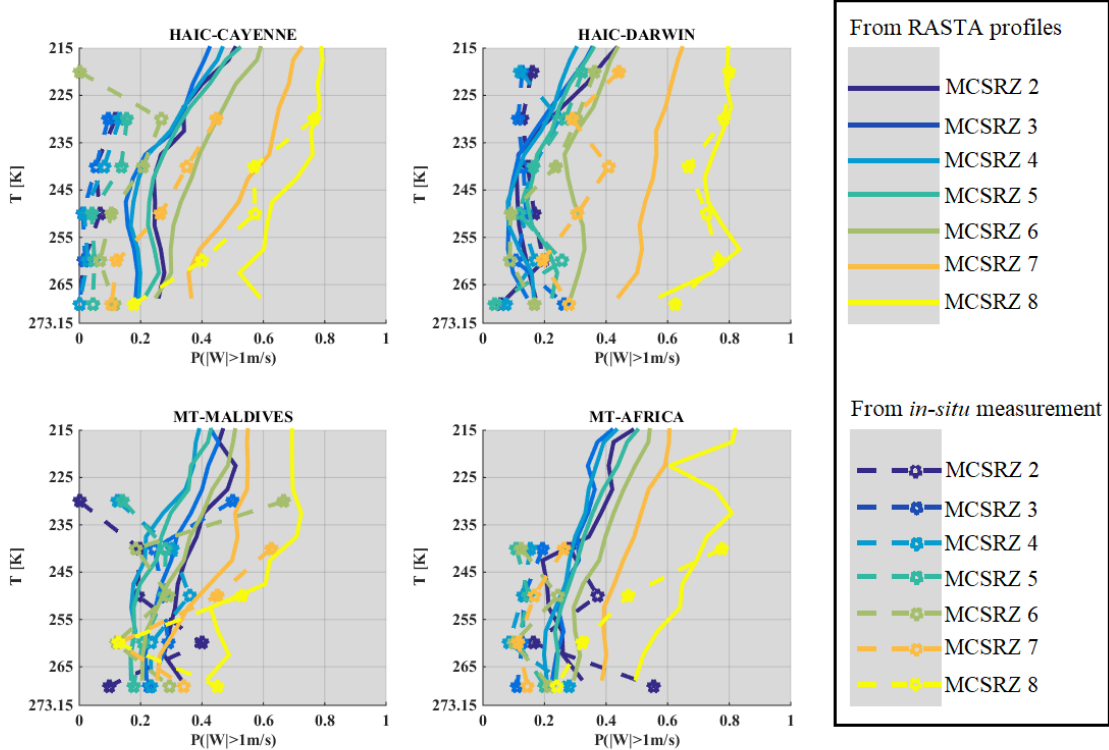


**Figure 4: Probability to observe vertical velocity with absolute magnitude larger than  $1\text{m/s}$  in each MCS reflectivity zone (MCSRZ; color scale) for measurement from the radar Doppler RASTA in solid lines and in dashed lines with stars marker for in-situ measurement.**

In Figure 4 we show that probabilities to observe  $|w_{\text{ret}}| \geq 1\text{m s}^{-1}$  are highest for MCS reflectivity zones 8 then 7 and 6, meaning that these MCS reflectivity zones tend to be more impacted by vertical movement (convective areas of MCS), than it is the case for other MCS reflectivity zones. Also, these probabilities generally increase with altitude for all airborne campaigns. Which meet the conclusions from Figure 3. Generally, in MCS reflectivity zones 5, 4, 3, and 2, the probabilities  $P(|w_{\text{ret}} \geq 1|)$  as a function of  $T$  are close to each other with a decreasing trend as reflectivity decreases, except for the Maldives campaign. Statistically, MCS reflectivity zones 8 and 7 represent for all 4 datasets the most convective part of observed MCS and the lower reflectivity zones the stratiform part with significantly lower vertical wind speeds.

*As a conclusion, at a constant altitude largest Z tend to be related with largest probabilities to observe vertical movement (downward or upward). In other words, MCS reflectivity zones 7 and 8 are good candidates to represent observations in the convective area of MCS or closer to the most convective part of MCS.“*

We add a sub-section in the end of section 5 (note that a new version of section 5 is written to satisfy comment of reviewer R2; see answer to reviewer 2) specific on the topic of impact of vertical velocity on ice microphysic (R1#4).

“

### **5.6 note on the impact of vertical movement on ice microphysic**

*This section discussed about the investigation performed about the impact of vertical velocity on the ice microphysical parameters presented earlier in this section 5. We separated the merged dataset in three sub-datasets such: i)  $w < -1\text{m/s}$ , (ii)  $-1\text{m/s} < w < 1\text{m/s}$  and (iii)  $w > 1\text{m/s}$ . Then, median relative difference for the three conditions and for each parameters presented in this section 5 were calculated and compared to the median relative difference when no distinction is performed as function of vertical velocity. Firstly, we noticed that MRD-X for the merged dataset and MRD-X for the second condition (i.e.  $1\text{m/s} < w < 1\text{m/s}$ ) are similar (MRD-X: X being used to replace IWC,  $\sigma$ , NT,  $NT_{50}$ ,  $NT_{500}$ ,  $\beta$ ,  $\alpha$ , max(Dmax)). Secondly, differences of MRD-X in updraft and in downdraft with regards to MRD-X for merged dataset and no vertical movement are visible. But most of the times these differences are not enough pronounced compared to measurement uncertainties ( $U(X)/X$ ).*

*Appendices B shows the Figures that shows when updraft have an impact on ice microphysic parameters for a given range of temperature and MCS reflectivity zones. So, Figure B1 shows MRD-IWC, Figure B2 shows MRD-NT and Figure B3 shows MRD-NT50. For the others parameters impact of updraft are uncommon.*

*It appears that updraft tends to impact mainly concentrations of small hydrometeors and IWC for some type of MCS and some MCS reflectivity zones. So for NT (Figure B2), we observe larger NT for updraft in MCS observed over Cayenne, Maldives and Niamey. For Cayenne, it appears in MCS reflectivity zone 5 and 6 for temperatures between 245K and 265 K with NT 2 to 3 times larger than NT for merged dataset. For MCS over Maldives, median NT are 5 times to 20 times larger than NT when there is no noticeable vertical movement in MCS reflectivity zones 6, 7 and 8. Finally for MCS over Niamey, we observe larger NT in updraft than NT for the merged dataset in MCS reflectivity zones 6 for T around 240 K and in MCS reflectivity zones 8 above the bright band. We have similar conclusions for  $NT_{50}$  (Figure B3), except that ratios between  $NT_{50}$  in updraft and  $NT_{50}$  when no updraft is smaller than the ratio between NT in updraft and NT when no updraft.*

*IWC are impacted by updraft, only for MCS over Cayenne, in MCS reflectivity zone 4, 5, 6 and 7. IWC in updraft tend to be larger about +50% than IWC when no updraft, except in MCS reflectivity zones where IWC are about 2 times larger in updraft than IWC when no updraft.*

*This investigation on the impact of updraft and downdraft on ice microphysics, shows that updraft may have an impact on concentrations of small hydrometeors and IWC. However, updraft does not impact all type of MCS in the same way. So, there will need to perform deeper investigations on updraft impact.*

*Despites some noticeable impact of updraft on ice microphysic for our dataset, there is no significant (recurrence through all types of MCS or as function of T or Z) results to assess them for the merged dataset. So, the parameterization provided in the next section are not functions of vertical velocity. “*

**2) The discussion in several places talks about the importance of crystal shape, simulations using oblate spheroids, aggregation and the various mass-diameter relationships that depend on particle habit; however, even though in all four projects the 2D-S is used, an OAP with 10  $\mu\text{m}$  resolution, there are no images shown or used in this analysis. This is a large omission of the most valuable piece of information that is available in this data set and would address a number of the questions that are raised hypothetically.**

It is not an omission, shape of hydrometeors is not the topic of this study. We study bulk ice microphysical properties, and mass-size relationship in a way to focus on more general tendencies.

But to study variability of mass-size relationship, we use images of 2D-S and PIP to do our statistics and calculate the surface-size and perimeter-size relationships as it is describes in Fontaine et al., (2014) and Leroy et al., (2016). This, to deduce the exponent of mass-size relationship Beta and then study the variability of crystals shape through it (see Fontaine et al., (2014) and Leroy et al., (2016)). As this study is focused on bulk parameters; parameters summed over the size of hydrometeors. We study, the variability of shapes of hydrometeors through the variability of Beta in the 4 datasets. Moreover, the datasets contains some millions of images, our thought is that showing randomly some images even taken at each level and as function of radar reflectivity would have no statistical

meaning for our study and would make the paper less clear as it contains already a lot of figures. However, this study is not scientifically exhaustive concerning the datasets we are using and future publications could be dedicated to images only.

#### **Others reviewer's comments in supplement.**

**Line 8 page 2:** Instead of relative terms like "large" and "small", please list the actual size ranges for reference further in the study.

We propose to rephrase this section (R1#5).

"A number of studies (Gayet et al., (2012); Lawson et al., (2010) and Stith et al., (2014)), demonstrate the presence of different type of ice hydrometeors in evolving MCS. In the active convective area, large super cooled droplets larger than 500 $\mu\text{m}$  until 3mm, were observed near -4°C and rimed ice hydrometeors about the same size below -11°C. Also at -47°C large rimed particles about 2-3mm from updraft regions coexisting with small ice crystals about 100 $\mu\text{m}$  (pristine ice) were encountered. Near the convective zone of MCS (i.e fresh anvil) presence of pristine ice (about 100 $\mu\text{m}$ ), aggregates of hexagonal plates (about 500 $\mu\text{m}$  to 1mm) and capped columns (about 500 $\mu\text{m}$ ) has been reported (Lawson et al., 2010). In aged anvils, columns (~100 $\mu\text{m}$ ), plates (~100 $\mu\text{m}$ ), and small aggregates (about 200 $\mu\text{m}$ ) are observed near -43°C while large aggregates about 2mm and more are found at lower altitudes (-36°C). Also in the cirrus part of MCS bullet-rosettes about 500 $\mu\text{m}$  and less (more common for in situ cirrus (Lawson et al., 2010)) and chain-like aggregates from 100 $\mu\text{m}$  to about 1mm are found (aggregates of small rimed droplets caused by electric fields: Gayet et al., 2012; Stith et al., 2014)."

**Line 24 page 3:** The term "barycentre" is not one that is commonly used in this context, and considering you use Dmax in one case, and radius in the other, I think a very brief clarification would be useful here.

As the processing of OAP for our dataset is presented and described in Leroy et al., 2016. We use the same definition of Dmax given in Leroy et al., 2016 (end of page 3): "The definition used in this study also varies from the others above in that Dmax is the largest length through the center of the particle image". This definition comes with a detailed figure, the Figure 1 in Leroy et al., 2016 (see below).

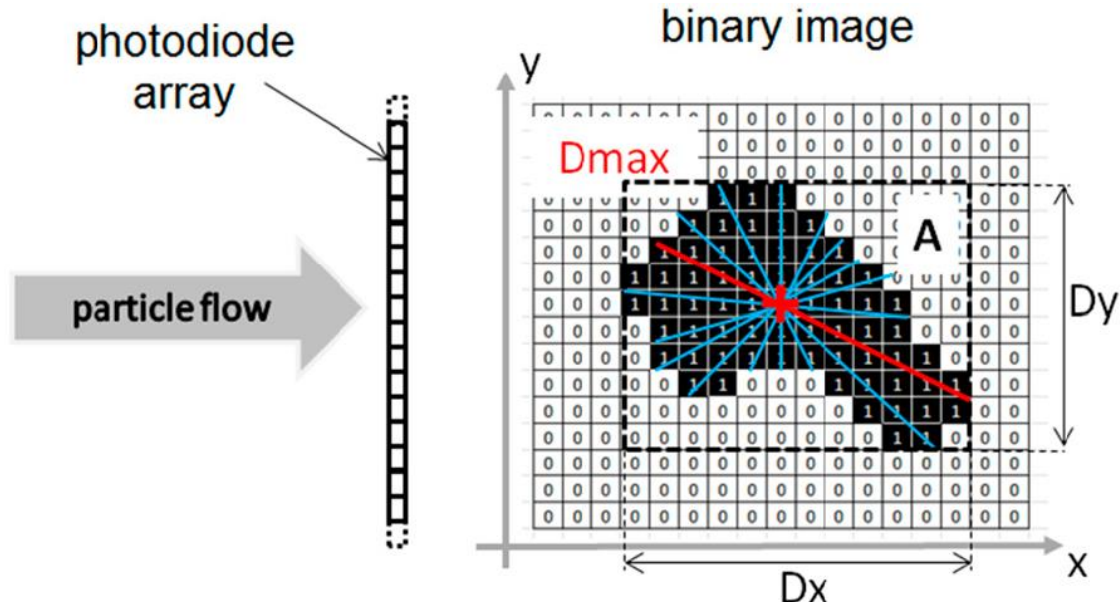


FIG. 1. Definition of particle dimensions that are extracted from OAP binary images. Blue lines illustrate some possible diameters passing through the center of the image, whereas the red line highlights the longest one, which is defined in this study as the maximum dimension.

We suggest to rephrase this section as (R1#6):

"Both OAP probes record black and white images of hydrometeors with a resolution of 10 $\mu\text{m}$  and 100 $\mu\text{m}$  (2D-S and PIP, respectively). They are used to derived the size of hydrometeors (Dmax [cm] in this study), their projected surface (S [cm<sup>2</sup>]), their concentrations as a function of their size (N(Dmax) [#/ $\mu\text{m}$ ]). The sizes of hydrometeors span from 10  $\mu\text{m}$  to 1.28 cm with Dmax calculated as a function of the projected surface of hydrometeors (taking the maximum of radius passing through its barycentre; see Figure 1 in Leroy et al., 2016)."

**Line 26 page 3: How is IWC derived from the OAPs, i.e. what ice density or what mass-diameter relationship is used?**

**And**

**Line 27 page 3: This is quite confusing. What do simulations of the reflectivity factor have to do with retrieving IWC from the IKP-2?**

First of all, IWC are not retrieved from OAP only by taking a mass-size relationship from former studies, nowhere in this paper there is a mention of such methodology.

In fact, there is two type of IWC used in this study. For both HAIC-HIWC campaigns, IWC was measured directly with the IKP-2 probes. It measures Total water content and then deduce IWC knowing relative humidity. For Megha-Tropiques we use simulations of radar reflectivity factors using PSD, and aspect ratio calculated with OAP (Fontaine et al., 2014 & 217) to retrieve IWC. The accuracy of the method to retrieve IWC from Z has been evaluated and tested in Fontaine et al., (2017).

We propose to rephrase this section (R1#7):

*“During both HAIC-HIWC campaigns, the IKP-2 probe was used to measure total condensed water, composed exclusively of ice water content (IWC [g m<sup>-3</sup>]) and water vapour, then IWC were deduced using in-situ measurement of relative humidity. However, IWCs < 0.1 g m<sup>-3</sup> are not considered in this study, due to IKP-2 uncertainties particularly important for low IWC measurements (see Strapp et al. 2016a). For both Megha-Tropiques campaigns, IWC was retrieved using simulations of the reflectivity factor Z, thereby using the approximation of ice oblate spheroids (Fontaine et al., 2017; Fontaine et al., 2014). Results about accuracy of IWC retrieved from this method with regards to IKP-2 measurement are discussed in Fontaine et al., (2017).”*

**Line 6 page 4: In the introduction and abstract 215K is listed as the minimum T**

Indeed, more clarification are needed concerning the temperature range of the dataset.

We propose to rephrase the sentence line 35 page 2 “The statistical analysis includes more than 55844 data points of 5 s measurement duration in the temperature range from 215K to 273.15K.” By (R1#8):

*“Our statistical analysis is performed on cloud radar Doppler measurement and in-situ measurement. Cloud radar measurements include more than one million of data points of radar reflectivity factors and retrieved vertical velocities spanning from 170K to 273.15K (Temperature profiles from RASTA are calculating using re-analysis of ECMWF). And in-situ measurements include 55844 data points of 5 s duration in the temperature range from 215K to 273.15K.”*

**Line 2 page 5: Where do you discuss how ice is differentiated from liquid?**

Indeed, few unclear words mention it at line 24 page 12. We propose to add some explanation at the end of section 2 (R1#9).

*“Moreover, investigations have been performed to detect supercooled water using Rosemount icing detector (Baumgardner and Rodi 1989; Claffey et al. 1995; Cober et al. 2001) and Cloud Droplet Probe measurement. Few cases of super cooled water were detected and remove from the dataset (Leroy et al., 2016). Hence, the dataset used in this study is using exclusively data collected where only ice particles were measured.”*

**Line 12 page 8: This section is very confusing on many levels. First of all, it is not at all clear where the IKP measurements are. The text says "Figure 5" but there are 5 panels of Fig. 5.**

IKP measurement of HAIC\_HIWC and retrieved IWC of Megha-Tropiques are merged, then statistic (calculus of median, 25<sup>th</sup> and 75<sup>th</sup> percentile) as function of temperature and MCS reflectivity zones are performed on this merged dataset. Which is done for all other microphysical parameters used in this study.

We propose to rephrase the beginning of this section (R1#10).

*“This section discuss about IWC measured during HAIC-HIWC project and the IWC retrieved for the Megha-Tropiques project. IWC from the four dataset were merged to calculate the main statistic (merged dataset). Figure*

5 shows median IWC for the merged dataset as a function of T and as function of MCS reflectivity zones (colored lines). Solely ... ”

**Secondly, the IWC is apparently being derived from the Z using T-matrix simulations but this is making a huge assumption about the habits of the ice crystals and seems to ignore the possibility of mixed phase.**

We use IWC retrieved from radar reflectivity factors only for the Megha-Tropiques project. There is no retrieved IWC in mixed phase condition. More details on this methodology can be find in Fontaine et al., (2014 and 2017).

To the end of the added paragraph noticed for the comment line 2 page 5, we propose to add (R1#11)

“Also, retrieval of IWC for the Megha-Tropiques project were not performed in mixed phase conditions (more details in Fontaine et al., (2014) and (2017)).”

**It seems that uncertainty is only being based on uncertainty in OAP measurements but the uncertainty in derived IWC simulations is certainly much larger than the uncertainty in the OAP derived IWC.**

There is uncertainty specific to measurement from IKP-2 probes available only for HAIC-HIWC project that vary as function of T. And uncertainty specific to the retrieval method used for the Megha-Tropiques project. This method is described in two publications Fontaine et al., (2014) and (2017). Here, we using the uncertainty with regards to measurement of IKP estimated in Fontaine et al., (2017).

**Thirdly, this figure should be presented as two figures, 5a as one and 5b-e as another. Not only is it too cluttered but it is very difficult to see the details in the individual panels.**

New figures are made (see revised manuscript), taking into account this comment and the comment of the second reviewer using colour blind-friendly colour schemes.

**Line 26 page 8: I cannot understand what is being described here, i.e. what is the uncertainty from the IKP and what is the uncertainty from the T-matrix simulations. Please clarify.**

As IKP-2 was used only for HAIC-HIWC its uncertainty is only plotted on Figure 5-b) and Figure 5-c), this uncertainty vary as function of T and is showed by the grey band in Figure 5-b) and Figure 5-c). The uncertainty of retrieved IWC is only shown on Figure 5-d) and Figure 5-e), as IWC for Megha-Tropiques are retrieved from the method described in Fontaine et al., (2014) and (2017). Note that Figure 5-b, c, d, e) wil become Figure 6-a, b, c, d) in the new manuscript.

We propose to rephrase the under lighted text with (R1#12)

“Figure 6 shows MRD-IWC for the four different campaigns. It is necessary that we recall that median IWC as function of T and MCS reflectivity zones are calculated using a merged dataset where there are IWC from direct measurement and retrieved IWC from Z and PSD (Fontaine et al., 2017). Then, there is two different uncertainties to consider to evaluate the MRD-IWC in each campaigns. Firstly, for Darwin and Cayenne campaigns the IWC were measured with IKP-2 probe (direct measurement) with an uncertainty on measured IWC increasing with temperature (~5% at 220K and ~20% at 273.15 K; Strapp et al., 2016). Secondly, for Niamey and Maldives IWC were retrieved using the method described by Fontaine et al., (2017) (indirect measurement) with an uncertainty with regards to the IKP estimated by about ±32%. Hence, in Figure 6-a) and Figure 6-b) the grey band area show the uncertainty of the IKP-2 probe that was used for Cayenne and Darwin campaigns. While in Figure 6-c) and Figure 6-d) the grey band area describe the uncertainty on the retrieval method for IWC that was used for datasets of Niamey and Maldives.

Note that confidence in direct bulk IWC measurements from the IKP-2 is significantly higher than in indirect IWC calculations from the retrieval method (Fontaine et al., 2017).”

**Line 16 page 9: These dashed lines are the same, at least on this figure, cannot differentiate dashed from dot-dashed.**

A new figure 5 is performed. Median IWC for merged dataset (black solid line), and for each campaigns are removed (other black dashed and dotted lines with markers). Then, the curve for the Heymsfield et al., (2009) is now plotted with a black solid line.

**Line 5 page 10: Are these in T bins of 10°C?**

Yes, statistics are performed on 10°C bins.

**Line 16 page 10: This is an important point to be addressed, how important are the < 100 um particles?**

The contribution of particles smaller than 100 $\mu\text{m}$  on the visible extinction is about 2% (median) in the range T [235K; 273.15K] and 10 % in the range T [215K; 225K]. Statistic calculated aver all the merged dataset (see figure R14 below).

We propose to rephrase the sentence with this comment (R1#13).

*"Note, that if we took uncertainties for particles smaller than 100 $\mu\text{m}$  (with  $(U(D))/D=\pm 50\%$  and  $(U(N))/N=\pm 100\%$ ) the uncertainty on the calculation of  $\sigma$  would increase to  $\pm 122\%$ . The reason why we do not take into account uncertainty of smaller particle is due to that these particles contribute little to the visible extinction (2% in the range [235K; 273.15] and 10% in the range [215K; 225K])."*

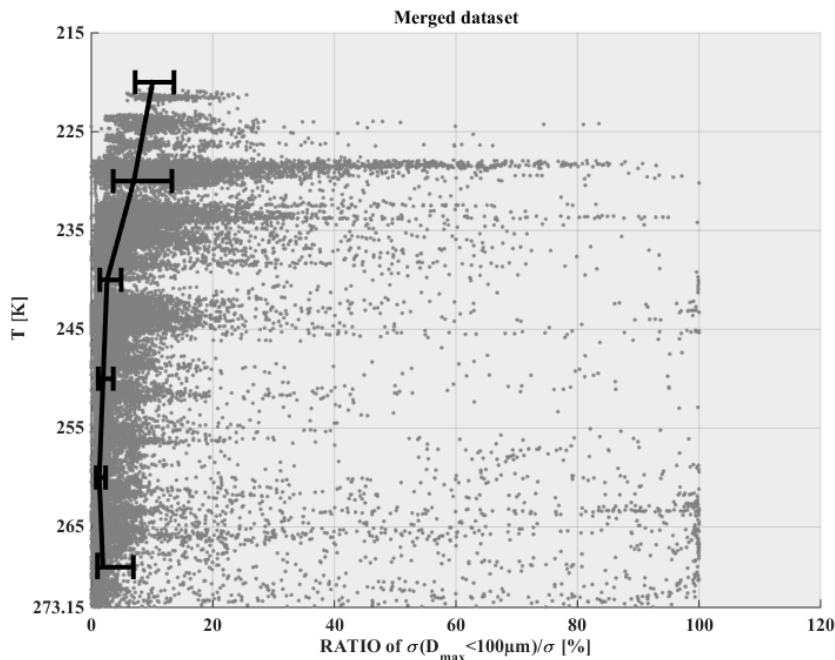


**Figure R 14: on x axis ratio of visible extinction calculated with particles smaller than 100 $\mu\text{m}$  over the visible extinction over all the spectrum of size of ice hydrometeors. On y axis the temperature. Black solid line represent median ratio. Statistic performed over the merged dataset.**

**Line 21 page 10: Why are there two lines?**

Be careful, there is only one grey dashed line that become a black solid line in the new figure.

**Line 24 page 12: This means few were detected or few removed? What about the radar data?**

See answer for the comment at line 20 page 6. This sentence is deleted in the new version of the manuscript as the topic is addressed earlier.

**Line 10 page 14: On what is this assumption based?**

I cannot remember why, this sentence appears here, or retrieve the context of this assumptions exactly. This sentence is deleted in the new manuscript.

**Line 20 page 14: This is possibly a result of sample sets that have Dmax>500 um. Where is this documented, i.e. data points at each T level at each Dmax condition?**

And

**Line 22 page 14: Exactly my point, what are the sample size of these conditions?**

For each parameters presented in this study, either for the merged dataset or the campaigns individually (for calculation of MRD-X), the calculation are performed with the same conditions. The samples in each conditions (T bins and Z bins) have the same size for all parameters. Indeed, data points are selected if they meet the

temperature and radar reflectivity criteria, but also the total concentration has to be positive (for  $D_{max} > 50\mu m$ ); mixed phased conditions being excluded. So, the size of the samples (i.e. same number of data points) for NT,  $NT_{50}$ ,  $NT_{500}$ , IWC, visible extinction, mass-size relationship coefficient, and  $\max(D_{max})$  are the same. So, if for a point there is no measurement of particle larger than  $500\mu m$   $NT_{500}$  is equal to  $0 L^{-1}$  which bring the  $MRD-NT_{500}$  to -100% for this point.

So sample size has no impact on the comparison of  $MRD-NT$ ,  $MRD-NT_{50}$  and  $MRD-NT_{500}$ , as it is the same for all of them.

We propose to add a comment to the end of section 4 (R1#14).

*"For each parameters presented in this study, either for the merged dataset or the campaigns individually (for calculation of  $MRD-X$ ), the calculation are performed with the same conditions. The samples in each conditions ( $T$  bins and  $Z$  bins;  $Z$  bins vary as function of altitude, i.e. MCS reflectivity zones) have the same size for all parameters. Indeed, data points are selected if they meet the temperature and radar reflectivity criteria, but also the total concentration has to be positive (for  $D_{max} > 50\mu m$ ); mixed phased conditions being excluded. So, the size of the samples (i.e. number of data points in each ranges of  $T$  and of  $Z$ ) for NT,  $NT_{50}$ ,  $NT_{500}$ , IWC, visible extinction, mass-size relationship coefficient, and  $\max(D_{max})$  are equal."*

#### **Line 4 page 15: Any aerosol measurements of any type on these flights? CN? PCASP?**

For sure there is no measurement of aerosol concentration of any types for the Megha-Tropiques campaigns. So, there is no general results that could be produced for this study.

#### **Line 19 page 16: Why CWC instead of IWC?**

Pure Writing mistakes.

#### **Line 18 page 17: Why speculate? With the OAPs, especially the 2D-S you have that information.**

Yes we have this information, here through the exponent Beta of the mass-size relationship. The perimeter-size relationship and surface size relationship that allow to calculate the exponent  $\beta$  of the mass-size relationship, are calculated using the images from the 2D-S and the PIP. Somewhere,  $\beta$  describe globally the variability of the shapes of hydrometeors.

We propose to add these two sentences line 30 page 15 (R1#15).

*"These two relationships are calculated using Images from 2D-S and PIP. Hence,  $\beta$  is a proxy parameter that describe the global (all over the size range of hydrometeors from  $50\mu m$  to  $1.2cm$ ) variability of the shape of the recorded hydrometeors during the sampling process (Leroy et al., 2014; Fontaine et al., 2014)"*

However, this section do not describe correctly the message that we wanted to give. So we propose to rephrase the part of the section 5.4 from the line 4 page 16 until the line 21 page 17 (R1#16).

*"In order to estimate the uncertainty on the calculation of  $\beta$  (grey band in Figure 14 (a), (b), (c), and (d), results from (Leroy et al., 2016) have been utilized, with  $U(\beta)/\beta = \pm 2.3\%$ . However, if we have calculated the uncertainty on retrieved  $\beta$  from the uncertainty on the measurement of the size and concentration of hydrometeors from OAP images, the uncertainty would have been by about 44%. In general,  $MRD-\beta$  in MCS reflectivity zones 8 and 7 tend to be in the range of  $U(\beta)/\beta$  assuming that  $\beta$  are similar for all observed MCS in the four campaigns for the conditions described by MCS reflectivity zones 7 and 8."*

*However, in MCS reflectivity zones 2 to 6  $MRD-\beta$  are more scattered around  $U(\beta)/\beta$  with sometimes larger  $MRD-\beta$  than uncertainty of  $\beta$ . Especially for MCS over Maldives and Niamey. Over Maldives at higher altitudes  $\beta$  tend to be smaller compared to the median  $\beta$  calculated for the merged dataset. While, MCS over Niamey tend to have  $\beta$  larger than median  $\beta$  calculated for the merged dataset.*

*Overall, the predictability of  $\beta$  coefficients as a function of  $T$  and MCS reflectivity zone remains challenging. We are aware of the fact that the power-law approximation has certain limits, trying to impose one single  $\beta$  to an entire crystal population composed of smaller (dominated by pristine ice) and larger crystals (more aggregation, also riming).*

For HAIC-HIWC data, coefficients  $\alpha$  are retrieved, while matching measured IWC from IKP-2 with calculated IWC thereby integrating PSD times  $m(D)$  power law relationship. For Maldives and Niamey datasets, coefficients  $\alpha$  are retrieved from T-matrix simulations of the reflectivity factor (Fontaine et al., 2017).

For both situation,  $\alpha$  calculation is solely constrained by the fact that the mass of ice crystals remains smaller or equal than the mass of an ice sphere with the same diameter  $D_{max}$ :

$$\alpha = \frac{IWC}{\sum_{15}^{12845} N(D_{max}) \cdot D_{max}^{\beta} \cdot \Delta D_{max}} \quad | \quad \alpha \cdot D_{max}^{\beta} \leq 0.917 \cdot \frac{\pi}{6} \cdot D_{max}^3 \quad [g \text{ cm}^{-\beta}]. \quad (6)$$

For the uncertainty calculation of  $\alpha$  we take the maximum value of  $\beta$  which is 3:

$$\frac{U(\alpha)}{\alpha} = \sqrt{\left(\frac{U(IWC)}{IWC}\right)^2 + 3 \cdot \left(\frac{U(D)}{D}\right)^2 \left(\frac{U(N)}{N}\right)^2} \quad (7)$$

Figure 15 shows median  $\alpha$  coefficients as a function of  $T$  and MCS reflectivity zone. As has been already stated in previous studies,  $\alpha$  is strongly linked to the variability of  $\beta$  (Fontaine et al., 2014; Heymsfield et al., 2010). Figure 15 compared to Figure 13 confirms that results for  $\alpha$  have similar trends as those discussed for  $\beta$ .  $\alpha$  vary from  $5.10^{-4}$  (in MCS reflectivity zone 2) to  $\approx 2.10^{-2}$  (in MCS reflectivity zone 8). In general,  $\alpha$  increases as a function of  $T$  for a given MCS reflectivity zone and also increases as a function of MCS reflectivity zone (and associated IWC) for a given  $T$  level. As already stated for the median exponent  $\beta$  in Figure 13, median  $\alpha$  in MCS reflectivity zones 4, 5, 6, 7 and 8 are more or less overlapping. ~~Median  $\alpha$  in MCS reflectivity zones 2 and 3 are shown for completeness reasons, however with less confidence as they are related to IWC generally smaller than  $0.1 g \text{ m}^{-3}$ .~~

From Figure 16(a) and Figure 16(b) we can note that even with a good accuracy of the measured IWC (from IKP-2;  $U(IWC)/IWC \approx \pm 5\%$  for the typical IWC values observed in HAIC-HIWC at 210K), the uncertainty of  $\alpha$ , is rather large which is mainly due to uncertainties in OAP size and concentration measurements. Taking into account the large uncertainty on the retrieved  $\alpha$ , we find that MRD- $\alpha$  for all 4 tropical datasets for MCS reflectivity zones 4, 5, 6, 7, and 8 are smaller than  $U(\alpha)/\alpha$ . For data from Niamey (Figure 16 (d)),  $\alpha$  tend to be larger than median  $\alpha$  for the tropical dataset (MRD- $\alpha$  not centered on 0, but shifted to positive values).

In previous sections, this study documented similar IWC values and visible extinction coefficients for a given range of  $Z$  and  $T$  and a clear increase of IWC and visible extinction coefficient from MCS reflectivity zones 4 to 8. The increase of  $\alpha$  and  $\beta$  with MCS reflectivity zones is not as much clearly visible, whereas at least  $\alpha$  seems to increase with temperature in different MCS reflectivity zones. And we cannot ignore that  $\alpha$  and  $\beta$  tend to be larger in MCS reflectivity zone 8 than in MCS reflectivity zone 4, especially at higher altitude. But, the increase of IWC and visible extinction with MCS reflectivity zone  $Z$  is not linked to an increase of the mass-size coefficients. This conclusion takes into account the variability of the mass-size coefficients shown by 25 and 75 percentiles. Moreover, ice hydrometeors habits describe with  $\beta$  in MCS reflectivity zone 4, 5 and 6 are different in MCS over Maldives and MCS over Niamey compared to MCS over Darwin and Cayenne (smaller  $\beta$  over Maldives and larger  $\beta$  over Niamey).

As visible extinction (hence projected surface) and IWC are similar for the same range of  $T$  and  $Z$  in all types of MCS, but the shapes of crystals might be different from one to another MCS location. Our assumptions is that the ratio of projected surface vs IWC is similar. In other words the density of ice per surface unity (or by pixels of projected surface) is similar as function of  $T$  and  $Z$  in all types of MCS even if there might be a possibility that the habit or the shape can be different (pure oceanic MCS vs pure continental MCS). Note that these assumptions are established for IWC larger than  $0.1 g \text{ m}^{-3}$ .”

#### **Line 14 page 18: How are aggregates being defined?**

Ice crystals aggregates are an agglomerate of pristine ice, the growth process of aggregates is leading by sedimentation of ice crystals (see Westbrook et al., 2004). But all the physic of aggregation process is still not well known; i.e. sticking coefficient for example.

We propose to rephrase this sentence (R1#17).

“In this section, it is shown that in the stratiform part of MCS, largest hydrometeors are larger in MCSs over Niamey than in other types of MCS, and tend to be smaller in MCS over Maldives Islands. Mainly, large crystals ( $D_{max} > 1mm$ ) are agglomerates of pristine ice crystals, for which the growth process is leaded by aggregations (by sedimentation) instead of vapour diffusion. Some large pristine ice were found in the dataset (especially over

Maldives see Figure 1 in Fontaine et al., 2014) but usually their size do not exceed 3 to 4 mm. So our observations of  $\max(D_{max})$  suggest that aggregation efficiency is different from one MCS type to another.”

**Line 18 page 18:** What is this analysis telling us that the IWC and visibility don't? The 2nd moment is visibility and the 3rd moment the IWC.

It might be true for the liquid hydrometeors, but theoretically there is no reason for ice hydrometeors that it is always true. This is why second Moment is discussed separately.

For the visibility we have:

$$\sigma = 2 \int_0^{\infty} N(D_{max}) \cdot e_s \cdot D_{max}^{f_s} \cdot dD_{max} = 2 \cdot S_T$$

Where  $f_s$  is the fractal dimension of the surface-size relationship that vary between 1 and 2 (see Mitchell 1996).

While for the second Moment we have:

$$M_2 = \int_0^{\infty} N(D_{max}) \cdot D_{max}^2 \cdot dD_{max}$$

However, when plotting  $\sigma$  versus  $M_2$  we can see that these two quantities are proportional. Indeed, Figure R15 tells us that there is a ratio between  $M_2$  and  $S_T$ . The computation of this ratio  $R_{M2-\sigma}$  is 0.72 (0.66, 0.68, 0.72, 0.75 and 0.78 for 10<sup>th</sup>, 25<sup>th</sup>, 50<sup>th</sup>, 75<sup>th</sup> and 90<sup>th</sup> percentiles) such:

$$R_{M2-\sigma} \cdot \sigma = \frac{\pi}{4} M_2$$

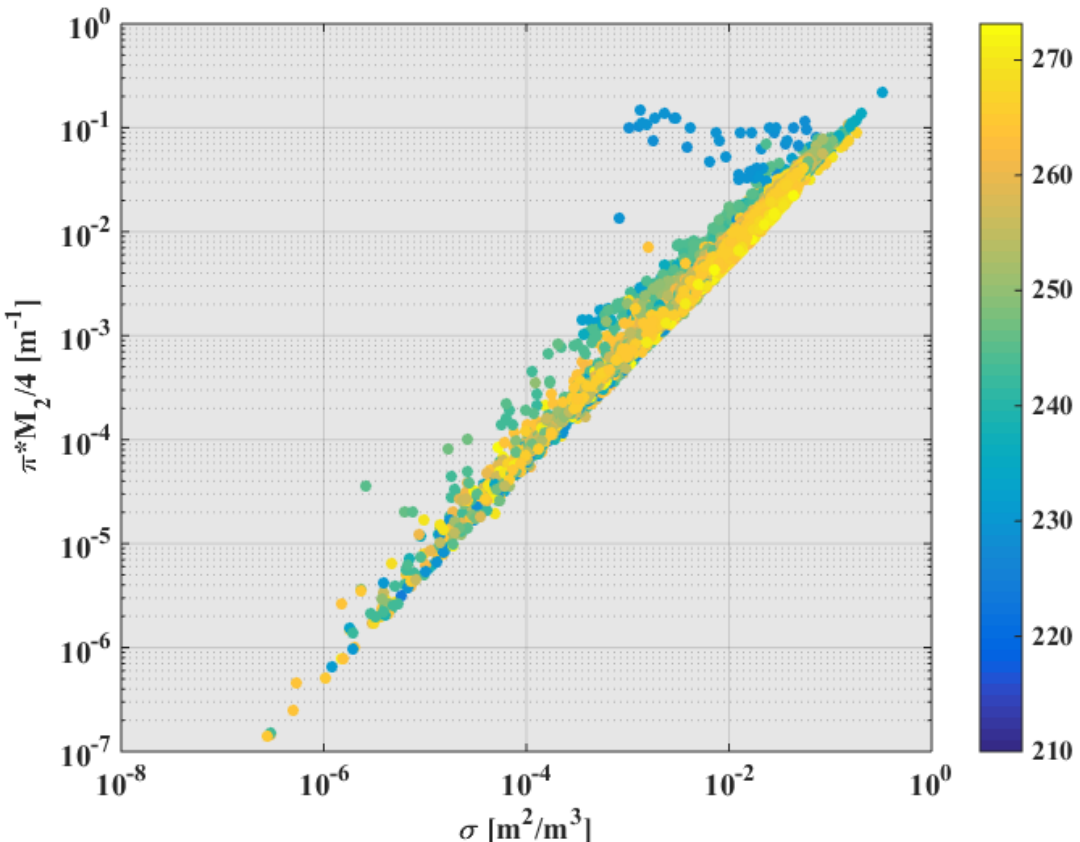


**Figure R 15:** on y-axis second moment of PSD ( $M_2$ ) as function of visible extinction of ice hydrometeors on x-axis. Data points are colored as function of in-situ Temperature in Kelvin.

Similar demonstrations can be done for the relationship between the third moment of PSD  $M_3$  and the IWC.

For the IWC we have:

$$IWC = \int_0^{\infty} N(D_{max}) \cdot \alpha \cdot D_{max}^{\beta} \cdot dD_{max}$$

Where  $\alpha$  and  $\beta$  are the coefficient of the mass-size relationship. For mass-size relationship  $\beta$  is rarely equal to 3 (except maybe for individual frozen droplets). And recent studies suggest that  $\beta$  (and  $\alpha$ ) could even vary as function of  $D_{max}$  (Erfani and Mitchell 2016; Coutris et al., 2017).

For the third Moment we have:

$$M_3 = \int_0^{\infty} N(D_{max}) \cdot D_{max}^3 \cdot dD_{max}$$

Figure R16, show that there is a trend of proportionality between IWC and the third Moment. But the spread is definitely too large to assume that third moment is equal to IWC or proportional to it.

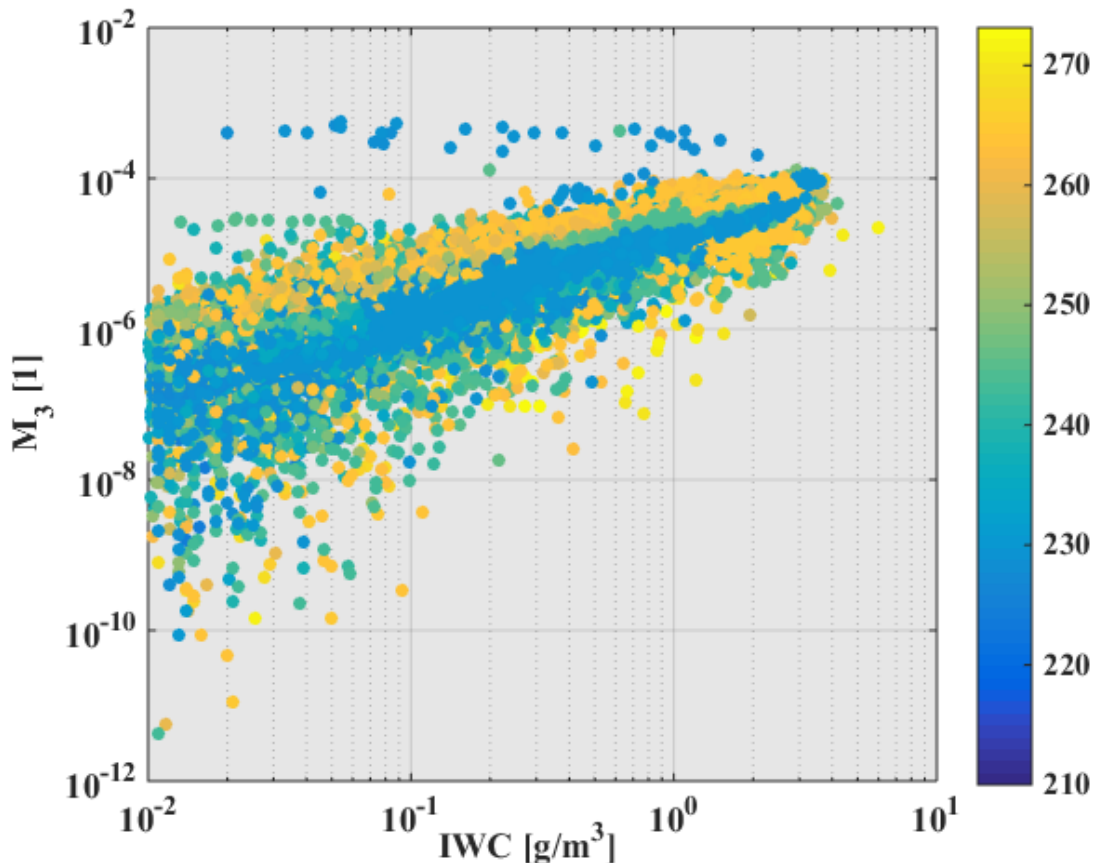


**Figure R 16:** on y-axis third moment of PSD ( $M_3$ ) as function of IWC on x-axis. Data points are colored as function of in-situ Temperature in Kelvin.

**Line 36 page 23: How does this differ from "Effective Radius"? This is really just the area weighted diameter**

Yes, but as this study provide an update of a former parameterization, we prefer to keep the same notation used in this former study (Field et al., 2007). Also, it can be find different definition of effective radius that are not exactly similar to the ratio of the third Moment and the second moment (see Delanoë et al., 2007; Heymsfield et al., 2002).

